Integrating urban recharge uncertainty into standard groundwater modeling practice: A case study on water main break predictions for the Barton Springs segment of the Edwards Aquifer, Austin, Texas

A Thesis
SUBMITTED TO THE FACULTY OF
UNIVERSITY OF MINNESOTA
BY

Kathryn M.L. Sinner

IN PARTIAL FULFILLMENT OF THE REQUIREMENTS
FOR THE DEGREE OF
MASTER OF SCIENCE

Rebecca L. Teasley

May 2017

Abstract

Groundwater models serve as integral tools for understanding flow processes and informing stakeholders and policy makers in management decisions. Historically, these models tended toward a deterministic nature, relying on historical data to predict and inform future decisions based on model outputs. This research works toward developing a stochastic method of modeling recharge inputs from pipe main break predictions in an existing groundwater model, which subsequently generates desired outputs incorporating future uncertainty rather than deterministic data. The case study for this research is the Barton Springs segment of the Edwards Aquifer near Austin, Texas. Researchers and water resource professionals have modeled the Edwards Aquifer for decades due to its high water quality, fragile ecosystem, and stakeholder interest. The original case study and model that this research builds upon was developed as a co-design problem with regional stakeholders; the model outcomes are generated specifically for communication with policy makers and managers. Recently, research in the Barton Springs segment demonstrated a significant contribution of urban, or anthropogenic, recharge to the aquifer, particularly during dry periods, using deterministic data sets. Due to social and ecological importance of urban water loss to recharge, this study develops an evaluation method to help predicted pipe breaks and their related recharge contribution within the Barton Springs segment of the Edwards Aquifer. To benefit groundwater management decision processes, the performance measures captured in the model results, such as springflow, head levels, storage, and others, were determined by previous work in elicitation of problem framing to determine stakeholder interests and concerns. Through additional modeling processes, this study compares the results of the previous deterministic model and the stochastic model to determine gains to stakeholder knowledge.

Table of Contents

List of Figures

List of Tables

List of Common Acronyms

BSEA: Barton Springs segment of the Edwards Aquifer

BSEACD: Barton Springs Edwards Aquifer Conservation District

BS GAM: Barton Springs Groundwater Availability Model

CI: Cast iron

DI: Ductile iron

DTM: Drought Trigger Methodology

GWM: Groundwater Management, a version of MODFLOW groundwater modeling Software

HCLOSE: Head-closure criterion for the solver package of MODFLOW

HFB: Horizontal Flow Barrier, an input file for MODFLOW

HydroID: Unique identifier for each MODFLOW model cell

IRF: Irrigation return flow

PVC: Polyvinyl chloride

SIP: Strongly implicit procedure, a solution method package of MODFLOW

QA/QC: The combination of quality assurance and quality control

USGS: United States Geological Surve

Chapter 1: Introduction

Groundwater depletion, or the long-term drainage of water from aquifers, presents international concerns regarding water stress, scarcity, sustainability, and land subsidence. Increasing global population, water quality declines, and climate change present additional challenges for groundwater resource management. In the United States alone, groundwater use increased dramatically in the 20th Century, particularly between 1950 and 1980 due to expanded use for irrigation, public supply, and industry (Hutson et al., 2004). From 1900-2008, groundwater depletion averaged 7.5 million acre-feet per year, totaling 0.81 billion acre-feet (Konikow, 2013). The maximum rates during the 1900-2008 time period occurred from 2000-2008, when average annual rates neared 20.3 million acre-feet. As of 2016, groundwater accounts for approximately 23% of freshwater use across the U.S., with agriculture as the biggest user at 68% (USGS, 2016).

While demands for groundwater increase, the aging distribution systems used to transport drinking water supplies presents additional challenges for water management. In the United States, much of the urban water distribution systems are beyond their 50-75 year life expectancy and elicit concern regarding break prediction and forecasted repairs (Duffy, 2016). Multiple studies on pipe break analyses exist in the literature and the integration of such research with industry provides both economic and ecologic benefit to communities. Conversely, leaky water mains may also artificially recharge an aquifer's groundwater supply, and the prediction of this water source also aids management decisions and policy.

The complexity of the interactions between precipitation, groundwater, surface water, and human-induced systems, such as a water and wastewater infrastructure, in addition to the uncertainties in the aquifer properties, make it difficult to effectively measure and predict the availability of groundwater resources. For this reason, groundwater managers often use computer models to analyze groundwater flow systems and the uncertain responses of aquifer stresses such as droughts, withdrawals, and contamination. Many traditional groundwater flow models are deterministic in nature, where defined model parameters will always produce the same output for a given input. For the uncertain

nature of water supply predictions, however, it is advantageous to integrate probabilistic randomness into groundwater flow models. This process, known as stochastic modeling, uses inputs defined by statistical parameters to produce a distribution of outputs, resulting in bounds of uncertainty for risk assessment and integration.

1.1 Motivation for Study

Increasing urbanization, climate change, and the ability to predict urban recharge within the context of uncertainty motivate this study. Recent research on the Barton Springs segment of the Edwards Aquifer focused efforts on accurately predicting recharge from artificial sources, including water and wastewater infrastructure and irrigation return flow (Passarello, 2011). The integration of urban, or artificial, recharge into the vetted BSEA groundwater flow model (Scanlon et al., 2001) by Passarello (2011) resulted in a significant contribution of research from artificial sources, particularly during dry time periods. The research presented in the study works towards developing a stochastic model for the BSEA through the quantification of artificial recharge from water distribution mains using break prediction.

1.2 Objective

The objective of this study is fourfold:

1. Develop a stochastic method to evaluate the effect of pipe break prediction on discharge at Barton Springs using the scenarios of vetted Barton Springs Groundwater Availability Model (BS GAM; Scanlon et al., 2001; Passarello, 2011)
2. Develop a MODFLOW Groundwater Management (GWM) model package for the BS GAM;
3. Maximize groundwater withdrawals in the Barton Springs segment of the Edwards Aquifer (BSEA) for increased future demand according to drought trigger constraints established by the BSEACD using the developed GWM model package; and

4. Evaluate groundwater management for stakeholders through the application of the performance criteria reliability and resiliency to aquifer demand, i.e. allocated withdrawals by the BSEACD, and maximum withdrawals achieved by GWM.

Chapter 2: Background

Several groundwater flow models have been created for the BSEA, yet none have yet to incorporate stochastic modeling or MODFLOW-GWM for optimization and management. The purpose of this chapter is to provide background information for this project and justify the research presented in this paper. Through the discussion of the study area, previously developed groundwater models, pipe break prediction models, and GWM optimization, this chapter provides the previous work relevant to the modeling packages developed in this project.

2.1 Study Area

The area of focus for this study is the Barton Springs segment of the Edwards Aquifer. The Edwards, or Balcones Fault Zone, Aquifer, one of the most prolific karst aquifers in the United States, is located in south central Texas along the Balcones Fault Zone (BFZ) in between the Edwards Plateau and the Gulf Coastal Plain. The Edwards Aquifer stretches 180 miles (290 kilometers) southwest to northeast from Kinney County to Hays County and supplies water to approximately 2 million people (Figure 1). Major cities in Texas on the aquifer include San Antonio and Austin. A groundwater divide at Kyle, Texas and the Colorado River separate the aquifer into three segments from south to north: the San Antonio segment, the Barton Springs segment, and the Northern segment. A groundwater divide at Kyle bounds the Barton Springs segment of the Edwards Aquifer (BSEA) to the south and the Colorado River in Austin serves as the northern boundary. The northeast and southwest portions of Barton Springs segment of the Edwards Aquifer lie in Travis and Hays Counties, respectively (Scanlon et al., 2001).

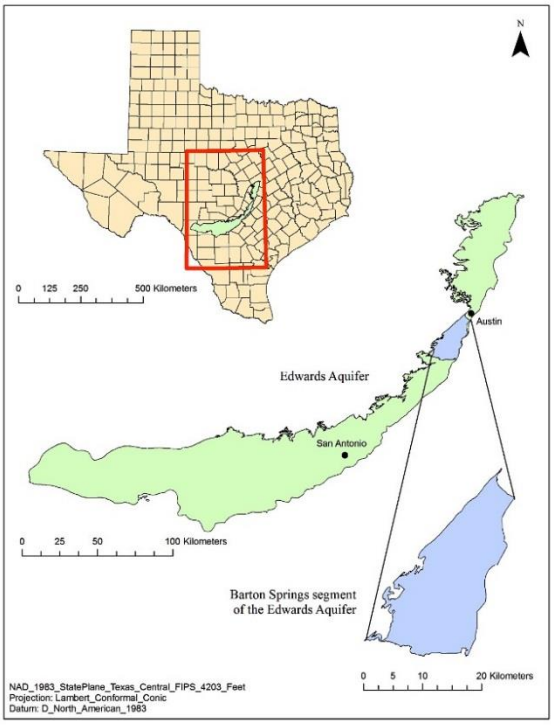

Figure 1. Site map of the study area (Passarello, 2011).

2.1.1 Physiographic Setting and Climate

Barton Springs is the smallest segment of the Edwards Aquifer and encompasses an area of 155 square miles (400 square kilometers) within the BFZ. The BFZ is an escarpment with northeast-trending, normal faults that provides an eastern boundary to the Edwards Plateau and a western boundary to the Gulf Coastal Plain, also known as the Blackland Prairies of Central Texas. In addition to the southern and northern boundaries, the Mount Bonnell Fault provides a no-flow boundary to the west (Senger and Kreitler, 1984) and a "bad-water" line provides the eastern boundary. The "bad-water' line actually represents a transition zone where the BSEA groundwater meets more brackish, saline water.

The Barton Springs study area has a humid, subtropical climate characterized by hot summers and relatively mild winters (NOAA, 2016). The region receives an annual precipitation of 33.4 inches (848 mm; 1981-2010) and averages an annual temperature of 69.4°F (20.8°C) (US Climate Data, 2016). The record high and low annual precipitations occurred in 1919 and 1954, with 64.7 in (1643 mm) and 11.4 in (290.1 mm), respectively

(NOAA, 2016). Climate data is from the Mueller/Camp Mabry station in Austin. Smith et al. (2013) note the study area has greater potential evaporation than precipitation. The Gulf of Mexico strongly influences precipitation in the area, with large summer rainstorms from May through July and the potential for tropical storms, depressions, and hurricanes from August through October. Peak rainfalls typically occur in May, when moisture off the Gulf of Mexico encounters fronts over Central Texas. The Balcones Escarpment creates an orographic effect, which exacerbates the rainfall and leads to some of the most intense rainfall per drainage area in the world (Smith et al., 2013). The intense storms, in addition to rapid runoff and low infiltration rates, lead to greater flooding in the Edwards Plateau than any other region in the U.S. (Caran and Baker, 1986).

Drought conditions and groundwater availability predictions present some of the main groundwater management challenges for the study area. Significant drought periods for the region occurred in the 1950s and again the late 2000s. 2011 is the driest and hottest year recorded for the study area. Although a report by Washington (2008) proposes most Global Circulation Models indicate a "general drying" of the Texas climate, other research on rainfall and streamflow conditions suggests otherwise (Nielson-Gammon, 2008; Singh, 2008; Leung, 2008; Hunt et al., 2012). As the last 30 years have been warming faster than the global average, Texas is likely to get hotter, regardless of changes to rainfall patterns (Nielson-Gammon, 2008; North, 2008). In general, climate change predictions, in addition to population growth are likely to dominate future groundwater challenges related to availability and spring flow (Mace, 2008; Laoiciga, 2008).

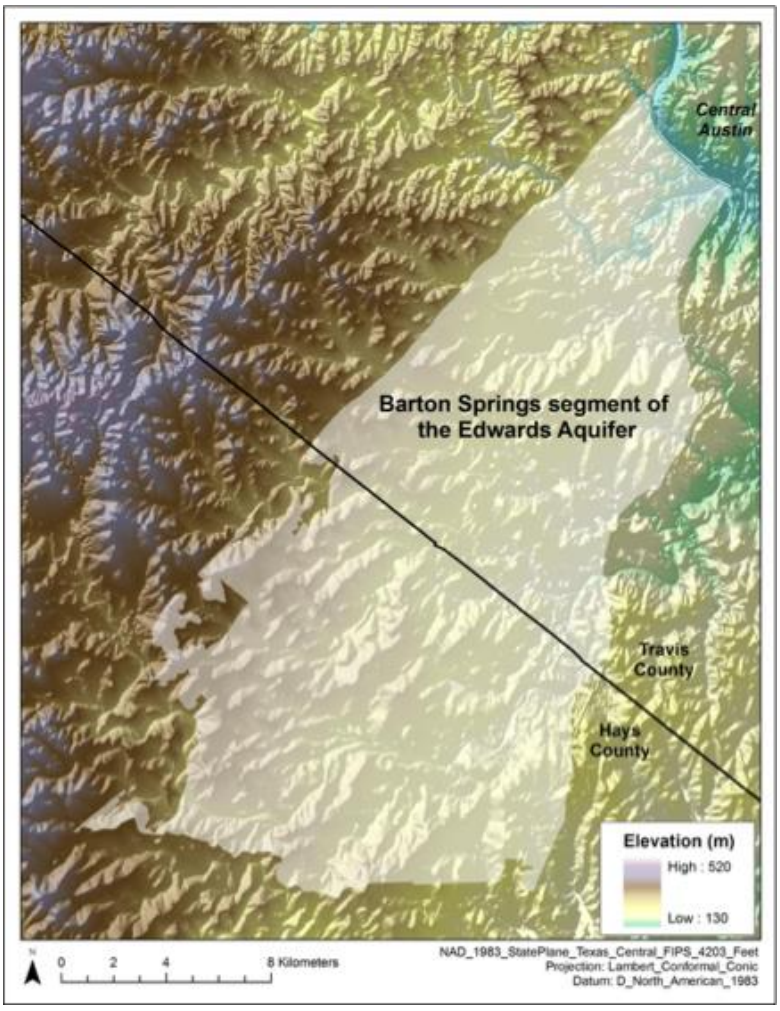

Figure 2**.** Topographic map of the BSEA (Passarello, 2011).

2.1.2 Aquifer Management

The BSEA provides the primary groundwater supply to approximately 60,000 people, including a portion of the City of Austin (BSEACD, 2010). By statutory mandate, the Barton Springs/Edwards Aquifer Conservation District (BSEACD) serves as the primary groundwater management body for the aquifer in regard to conservation, protection, and enhancement of groundwater resources (BSEACD, 2016). In addition to the Barton Springs segment of the Edwards Aquifer, the BSEACD also manages the portions of the Upper Trinity Aquifer that underlie the Edwards Aquifer in this region. Groundwater Management Area 10 provides oversight for the BSEACD and is administrated by the Texas Water Development Board. Maintaining spring flow and

predicting spring flow levels within the aquifer during drought periods present the key challenges of groundwater management for the District (Scanlon et al., 2003).

While the study area has history of rural domestic and agricultural water use, water from the BSEA and underlying Upper Trinity Aquifer are increasingly converted to residential and urban use, with the current primary use as domestic and public water-supply (BSEACD, 2016). As of 2008, the BSEACD permits approximately 1,230 wells with 100 permit holders. Without restrictions for drought, the wells within the district withdrew about 2.2 billion gallons, or approximately 6750 acre-feet, for the 2008 fiscal year from the Edwards and Trinity Aquifers (BSEACD, 2016).

With drinking water as the primary use of the Edwards Aquifer, it is designated as a sole source aquifer (SSA) by the United States Environmental Protection Agency (US EPA). By the EPA's definition, a sole source aquifer must supply at least 50 percent of the drinking water for the overlying service area and have no alternative sources of drinking water should the aquifer's water become contaminated (US EPA, 2016). The BSEACD is responsible for managing the groundwater resources of the aquifer and predicting available groundwater.

Groundwater availability, in addition to societal and environmental value, drive aquifer research as the BSEA provides habitat for endemic endangered species, has SSA designation, and discharges into Barton Springs at Zilker Park, a natural recreational pool for the City of Austin. The BSEA serves as the critical habitat for two federally endangered species, the Barton Springs salamander, (*Eurycea sosorum),* and the Austin Blind salamander (*Eurycea waterlooensis*). The federally threatened Jollyville Plateau salamander (*Eurycea tonkawae*) is also endemic to the area, but lives in streams of northwest Austin and southern Williamson County in addition to Barton Springs, unlike the two endangered salamanders whose habitat are solely the BSEA pools (Austintexas.gov, 2016). The sole habitat for the Austin Blind salamander and the Barton Springs salamander are the four main springs of Zilker Park, a popular public swimming hole in Austin, Texas and the primary discharge location for the BSEA.

Texas Administrative Code Title 31, Part 10, Chapter 356.C requires groundwater managers within conservation districts and management areas to use groundwater

modeling to predict the long-term availability of groundwater (TWDB, 2016). In addition, the BSEACD manages groundwater levels on a short-term basis through a stream gage at Barton Springs and the head levels at the Lovelady Monitoring Well, known as the District's "Drought Trigger Methodology", or DTM. The BSEACD adopted its Drought Trigger Methodology (DTM) in 2006 to assess and predict drought status for Barton Springs. The DTM uses the 10-day running discharge average (cfs) at Barton Springs and the elevation level above sea level (msl) of the Lovelady monitoring well to assess drought conditions as one of the following statuses from wet to dry: none, alarm, critical, and exceptional (Figure 3; Smith et al., 2013). The BSEACD declared critical droughts with the DTM in 2006, 2008, 2011, and 2013.

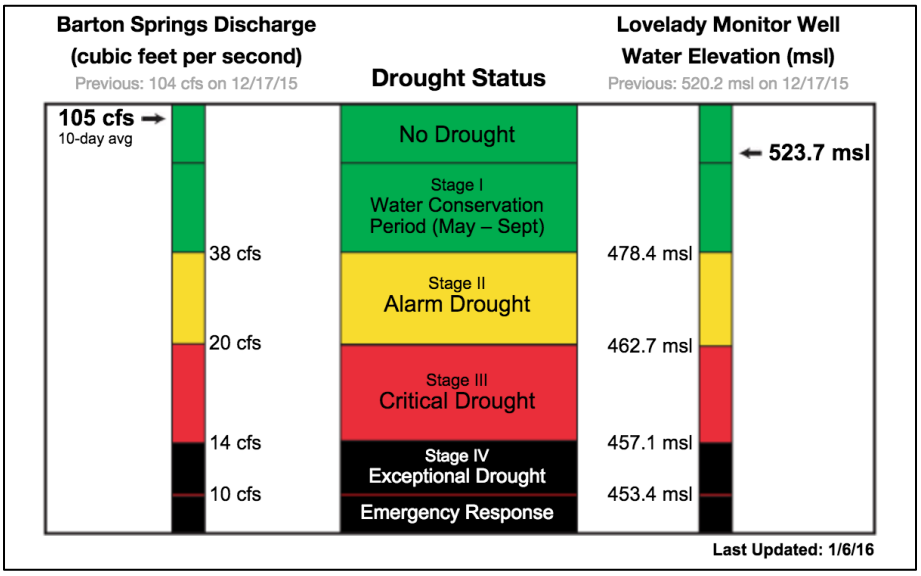

Figure 3. Drought Trigger Methodology for the BSEACD (BSEACD.org, 2016).

2.1.3 Geology and Hydrogeology

The Edwards Aquifer is composed of the Edwards Group of limestones deposited by warm, shallow seas 60-100 million years ago during the Cretaceous Period (Scanlon et al., 2001). Uneven dissolution of the limestone layers by groundwater circulation created the highly porous, karst nature of the aquifer, characterized by faults, fractures, caves, and sinkholes. Slade et al. (1985) determine 80% of the aquifer to be unconfined. Both the unconfined and confined portions of the Barton Springs segment of the Edwards Aquifer

are bounded below by the Glen Rose Formation. In the unconfined section, or the recharge zone, the Edwards Aquifer is exposed at the land surface. The Del Rio Formation serves as the aquitard for the top portion of the confined portion of the aquifer (Hovorka et al., 1998). The Trinity Aquifer, which consists of Upper, Middle, and Lower units, underlies the Edwards Aquifer and may be adjacent to it in areas due to faulting within the BFZ (Figure 4, Figure 5). The Upper Trinity Aquifer, part of the Glen Rose Formation, is hydrologically connected to the Edwards Aquifer, but contributes negligible groundwater flow for this study's modeling purposes.

The Barton Springs segment is bounded to east by the "bad-water" zone where total dissolved solids exceed 1000 mg/L, to the west by the no-flow boundary of the Mount Bonnell Fault, to the north by the Colorado River, and to the south by the groundwater divide near Onion Creek that is present during normal and wet hydrologic conditions (Figure 6; Hauwert, 2009). Recent studies found the groundwater divide transitions from Onion Creek to the Blanco River during drought conditions (Smith et al., 2012). The model for this study, developed by Scanlon et al. (2001) and altered by Passarello (2011), considers the southern groundwater divide boundary at Onion Creek (Figure 8).

Karst aquifers are known to have triple porosity, meaning the aquifer contains water in the rock matrix, fractures, and conduits, or openings formed through the chemical dissolution of limestone. Conduits within the Edwards Aquifer range in diameter from centimeters to meters (Edwards Aquifer Authority, 2016). Depending on the location, residence times within the aquifer can be anywhere from a few hours to years. The karst nature of the aquifer allows for a relatively large transmission of water and a response of water levels to temporal variations in recharge and localized pumping (Slade et al., 1985). Slade et al. (1985) noted the maximum fluctuations in water levels to be greatest within the confined area (40-120 feet) and smallest in the western portion of the aquifer near the recharge zone (<3-10 feet). Tracer tests by Hauwert et al. (2002a) indicate groundwater in the Barton Springs segment primarily flows north to northeast into Barton and Cold Springs.

General thicknesses of the Barton Springs segment of the Edwards Aquifer range from 568 feet (173 meters) on the east hydrologic boundary to 0 feet at the boundary of

recharge zone, which lies in the western portion of the aquifer. The aquifer is exposed at the surface in the recharge zone, which serves as a direct source of recharge due to infiltration (BSEACD, 2016). As much as 85% of recharge to Barton Springs is due to six losing streams, which originate west of the recharge zone in an area known as the contributing zone. These streams include Onion Creek, Bear Creek, Little Bear Creek, Williamson Creek, and Barton Creek, and are known to be "losing" streams as their flows eventually infiltrate into the aquifer through karst features and fractures (Slade et al., 1986). Of these six streams, Onion and Barton Creek contribute an estimated 53% of the recharge (Passarello, 2011). The remaining recharge sources include diffuse recharge, or the infiltration of precipitation directly into the groundwater. Slade et al. (1986) estimated the percentage of total recharge from diffuse sources to be approximately 15%, but Hauwert (2009) noted this percentage may be as much as 32%.

Passarello (2011) further illustrated the dynamic response of water levels in the karstic Edwards Aquifer through the quantification of artificial, or urban, recharge sources such as leaky utility lines and irrigation return flow in the Barton Springs segment. Spatial variability, such as land use and karst features, as well as temporal variations in rainfall, motivated Passarello's study. Passarello concluded total recharge from anthropogenic sources to provide 4% of the total recharge in the BSEA (1999-2009) ranging from <1 – 52% on a monthly basis with leaky utility lines as the overall greatest volumetric contribution.

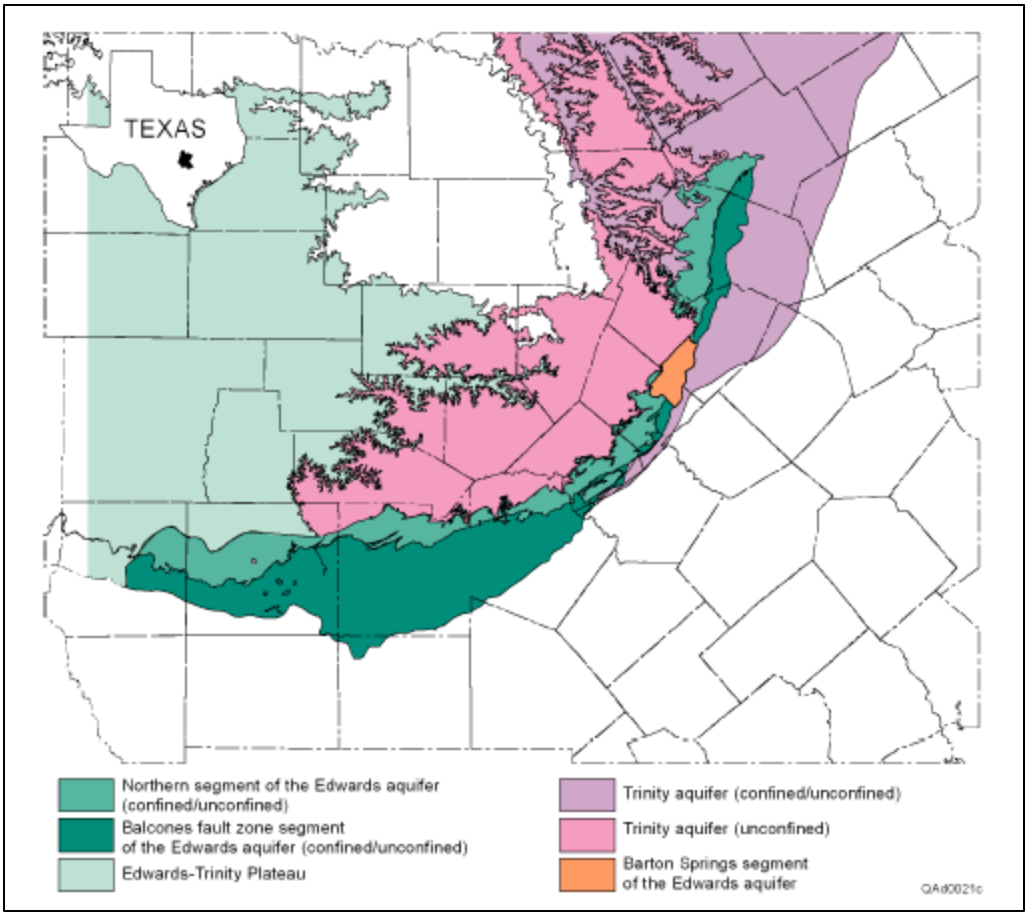

Figure 4. Geologic setting of the BSEA (Scanlon el al., 2001).

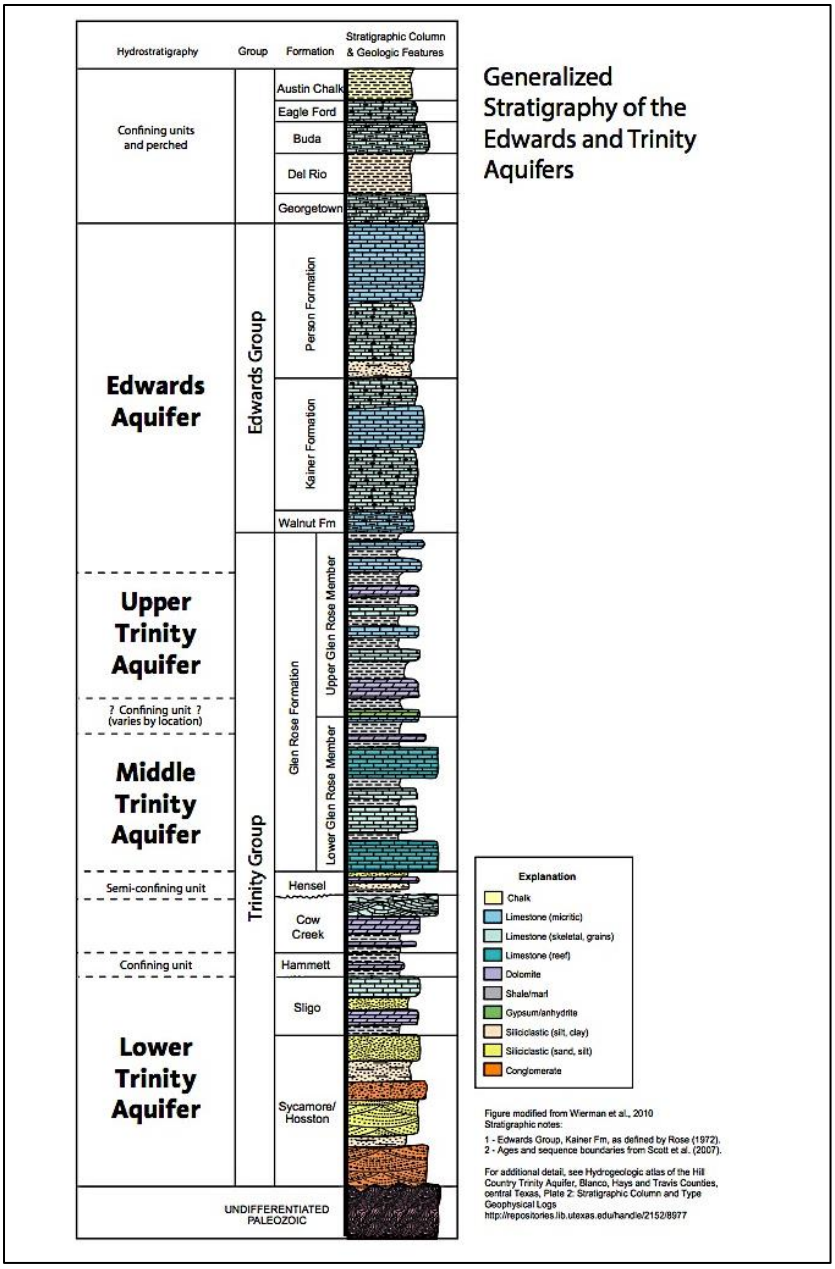

Figure 5. Geologic cross-section of the study area (BSEACD.org, 2016).

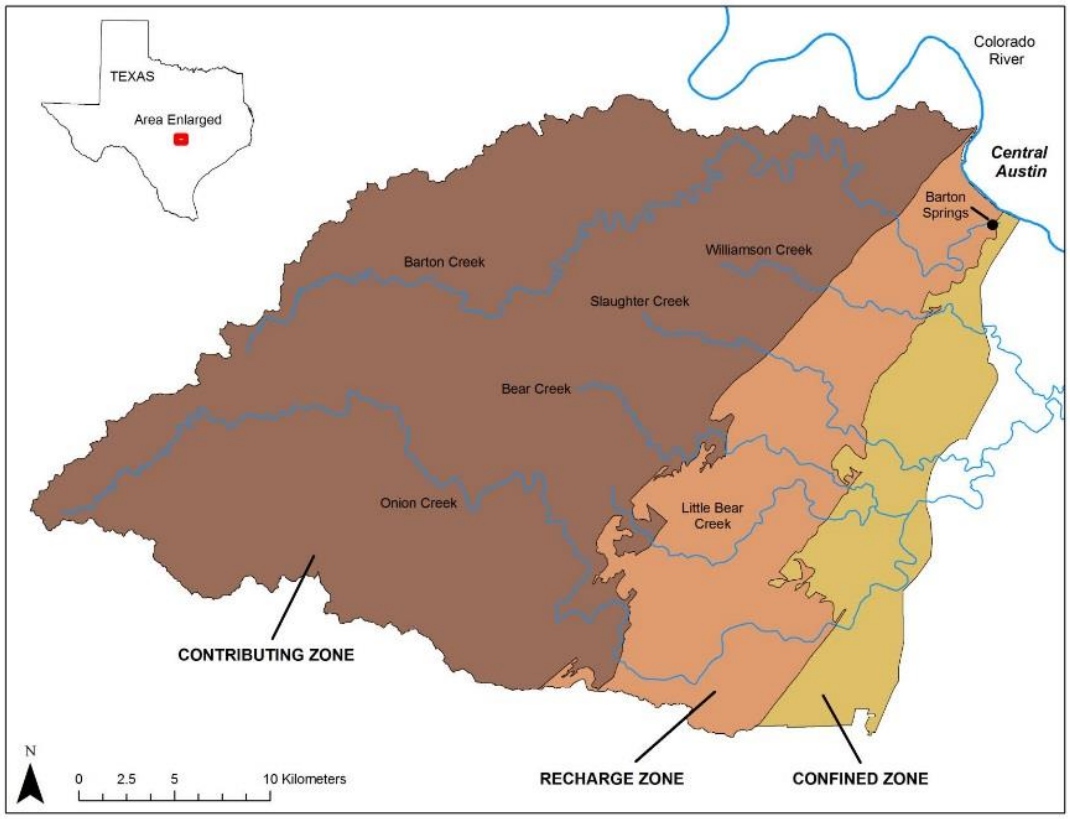

Figure 6. Map of hydrogeological zones and losing streams for the study area (Passarello, 2011).

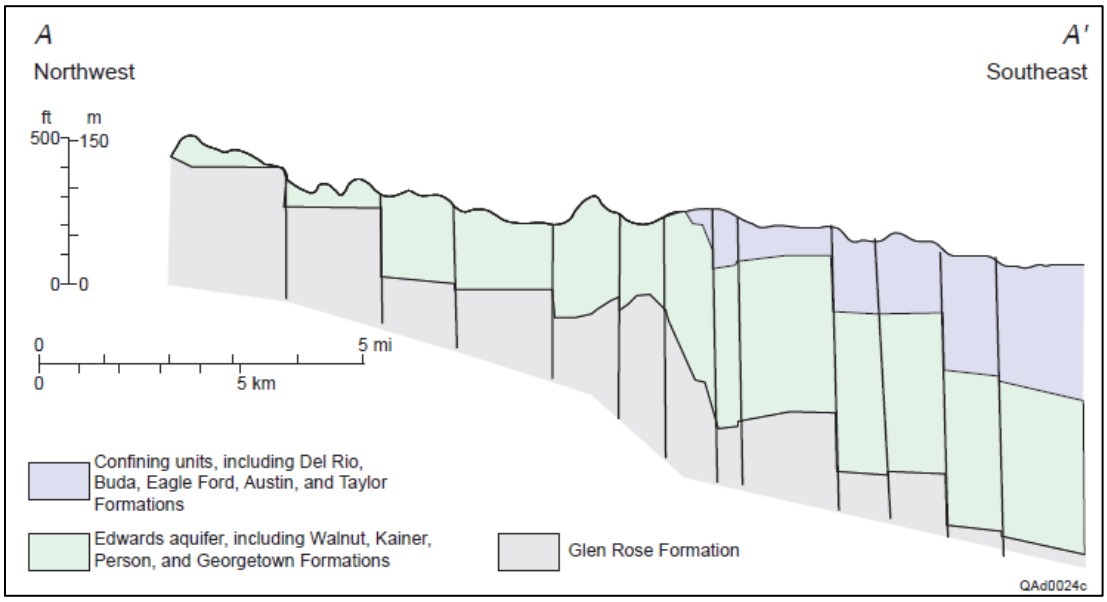

Figure 7. Geologic cross section of the Edwards Aquifer (Scanlon et al., 2001).

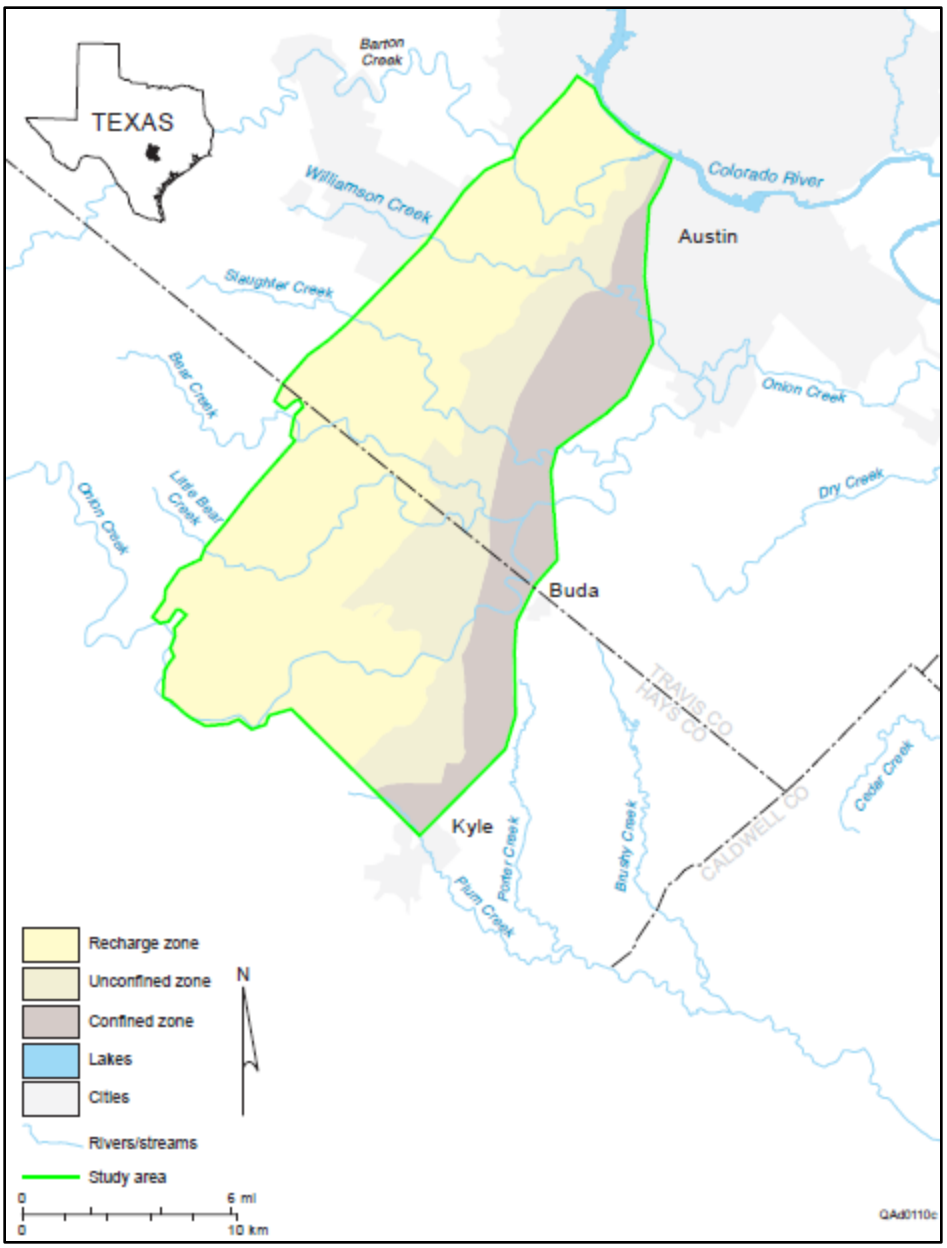

Figure 8. Hydrologic boundaries of the BSEA (Passarello, 2011).

2.2 Pipe Break Prediction

Drinking water infrastructure provides increasing challenges for American municipalities due to its aging mains, cost of repairs, and growing demand with the rise in urban and suburban populations. As the majority of American water mains were lain in the late 1800s, 1920s, and immediately following World War II, many of these distribution pipes have exceeded their expected lifespan of 50-75 years (Amwater, 2016). In their 2013 Report Card, the American Society of Civil Engineers (ASCE) awarded America's water infrastructure a D+, indicating a "poor and at risk" status due to the number of below standard, deteriorating, and outdated pipes (ASCE, 2013). According to the American Water Works Association (AWWA), the cost to serve the nation's water needs over the next twenty five years through restoration and expansion will exceed nearly one trillion dollars (AWWA, 2016). Although the ASCE stamps a poor letter grade on America's water infrastructure, they also note the high quality of drinking water across the United States. Integrating pipe risk analysis into water main assessment, hydrologic budgets, and water resource management may provide valuable for economic and conservation purposes. One of the primary objectives of this study is to determine discharge at Barton Springs based on the stochastic prediction of water main distribution breaks within the recharge zone of the Barton Springs segment of the Edwards Aquifer.

Several models have been created to assess the risk of pipe breakage (Shamir and Howard, 1979; Kettler and Goulter, 1985; Mailhot et al., 2000; Le Gat and Eisenbeis, 2000; Yamijala et al., 2009; Alvisi and Franchini, 2008). Pipe risk modeling is often classified as deterministic (Shamir and Howard, 1979; Walski and Pelliccia, 1982; Clark et al., 1982; McMullen, 1982; Kettler and Goulter, 1985; Jacobs and Kerney, 1994; Wang et al., 2009) or probabilistic (Cox, 1972; Marks et al., 1985; Andreou et al., 1987; Mailhot et al., 2000; Le Gat and Eisenbeis, 2000). In addition, risk assessment models use a variety of water distribution system data to achieve output predictions. While some models require pipe characteristic data ranging from one to over ten parameters such as pipe age, length, type, and soil classification, others do not require any pipe characteristics, but rather utilize break history data alone.

Due to the challenging nature of data access and availability in aging water distribution systems, the ideal model for this project requires access to a limited number of pipe characteristics. In addition, to facilitate the reproducibility of the method developed through this project with water resource professionals, the ideal model does not require intense statistical preparation. As a result of the desired specifications, the methodology chosen to assess stochastic artificial recharge due to the prediction of pipe failure probability is a series of regression models developed by Wang et al., 2009. Wang et al. (2009) developed a set of five models for water distribution mains composed of gray cast iron, ductile iron (with and without lining), PVC, and hyprescon (concrete) with Minitab (2002) statistical software. Using multiple linear regression analysis, the authors developed a best-of-fit equation for each pipe material based on the age, size (diameter, in millimeters), length in meters, and break history for water distribution mains in city of Ste-Foy in Ontario, Canada.

Wang et al. (2009) verified the regression models using a randomly selected sample from the municipality's data set and average validity and invalidity percentage models developed by Zayed and Halpin (2005), described in Equations 1 and 2:

$$AIP = \left(\sum_{i=1}^{n} |1 - \left(\frac{Ei}{Ci}\right)|\right) \quad (1)$$

$$AVP = 1 - AIP \quad (2)$$

where

AIP = average invalidity percent out of 100;

Ei = estimated/predicted value;

Ci = actual value

AVP = average validity percent

Average validity percentages for the regression models ranged from 50.0% (hyprescon) to 67.5% (gray cast iron), which the authors concluded as "fairly satisfactory." Wang et al. (2009) suggested low AVP values due to the limited size of each pipe type's data set. To test overall goodness of fit, the authors employed an F-test, which each model passed at

significance value, α, at 0.1, or 90%. Maximum and minimum R-squared values are 81.3 (hyprescon) and 65.0 (ductile iron, without lining), respectively (Table 1).

Table 1. Summary of break rate models (Wang et al., 2009).

Material	Total number of data points	Number of data points for model building	Number of data points for validation	Model equation	*R*-squared (%)	Significance test at α=0.1	Average validity percent (%)
Gray cast iron	476	381	95	$\text{Log}_{10}R=4.85-0.0206A+0.000245\ A^2+0.00281S-0.905\text{Log}_{10}L-1.40\ \text{Log}_{10}S$	68.9	Passed	60.8
Ductile iron (without lining)	187	149	38	$\text{Log}_{10}R=1.83-0.911\ \text{Log}_{10}L$	65.0	Passed	57.9
Ductile iron (with lining)	186	149	37	$\text{Log}_{10}R=3.36+0.000150\ L\times A-1.11\ \text{Log}_{10}-0.646\ \text{Log}_{10}A-0.254\ \text{Log}_{10}S$	71.5	Passed	64.3
PVC	136	113	23	$\text{Log}_{10}R=2.69-0.898\ \text{Log}_{10}L-0.745\ \text{Log}_{10}A$	78.9	Passed	67.5
Hyprescon	47	39	8	$\text{Log}_{10}R=1.81+0.00593\ L-0.000028\ L\times S-0.958\ \text{Log}_{10}L$	81.3	Passed	50.0

Wang et al. (2009) concluded for all pipe types of size 150 millimeters and 25 years of age, the number of breaks per kilometer decreases with increasing length from 100 to 600 meters (Figure 9). In addition, all pipe types with lengths less than 50 meters had higher break rates than longer lengths (Figure 10). The authors concluded break rates for 100 mm, 100 m long cast iron pipes increased with age after 45 years and had the highest break rates compared to other diameters examined (150, 200, 250, 300, 350 mm; Figure 11) and that 150 mm cast iron pipes of varying lengths (50, 100, 200, 400 m) also experienced increasing break rates with age (Figure 12).

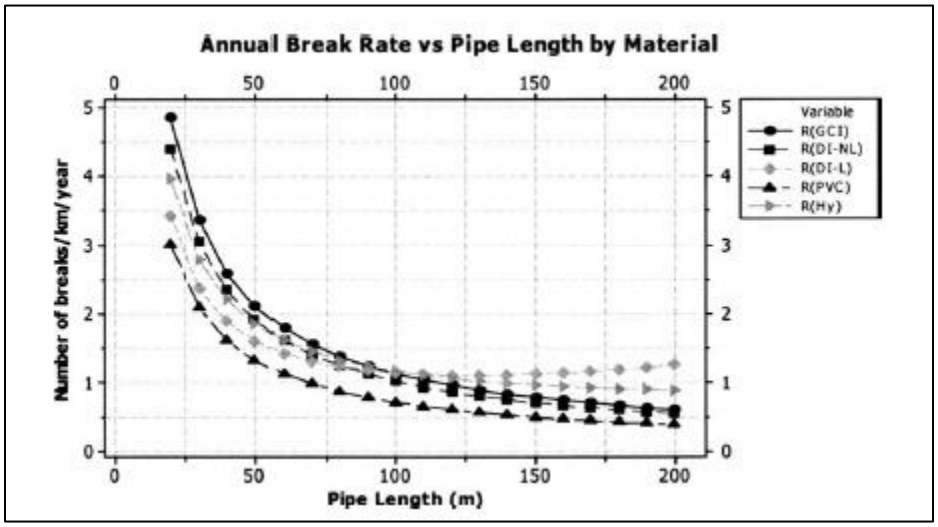

Figure 9. Break rate vs. length for all pipe types with 150 mm diameter and age 25 years (Wang et al., 2009).

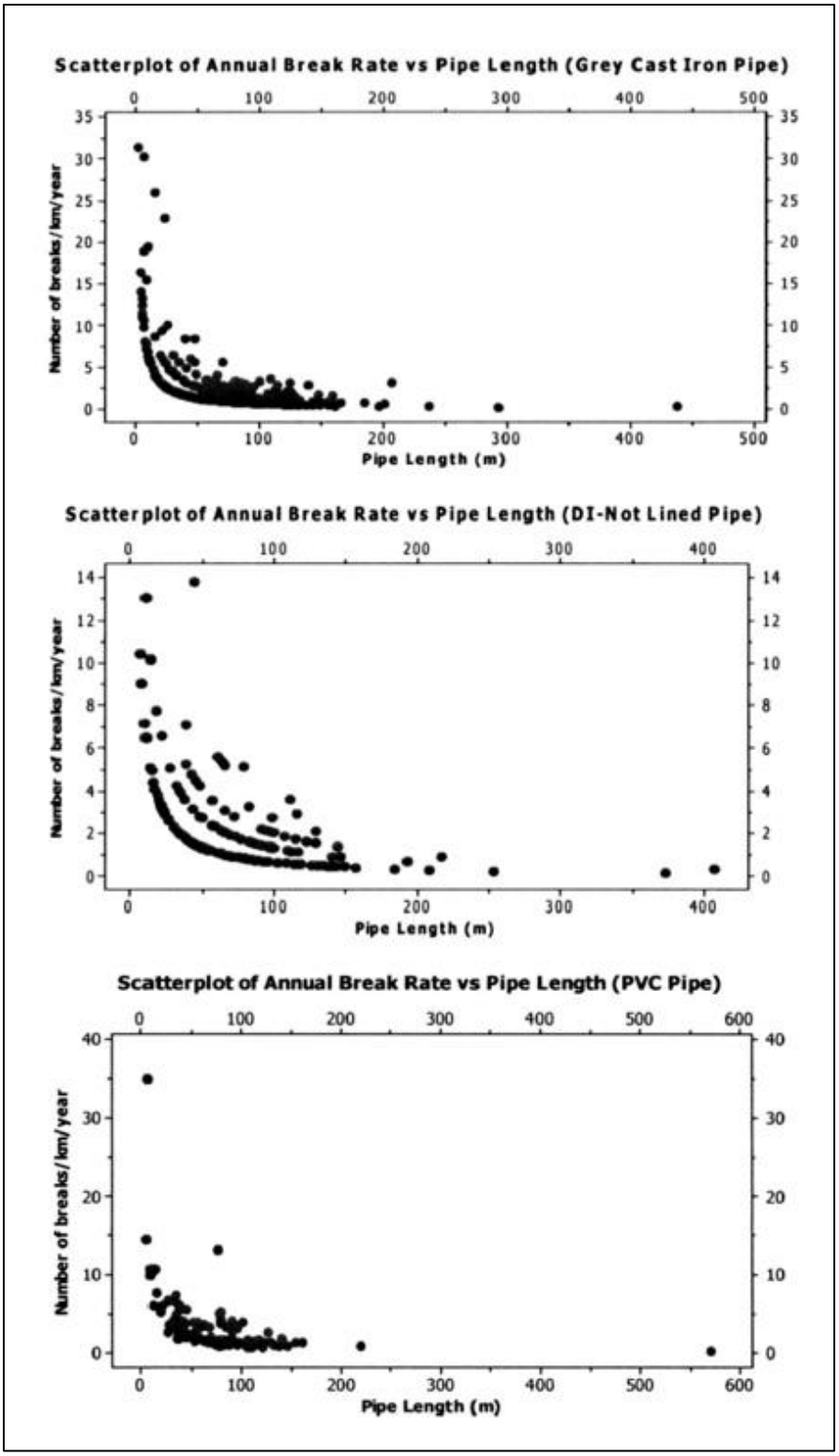

Figure 10. Scatterplots of annual break rates vs. length for CI, DI, and PVC pipes (Wang et al., 2009).

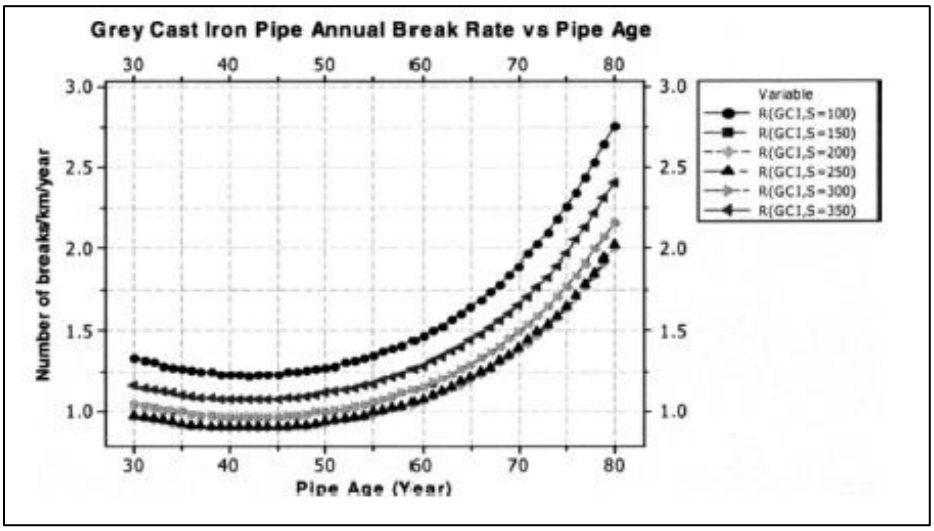

Figure 11. Break rates vs. age for cast iron pipes with 100 meter length and varying diameter (Wang et al., 2009).

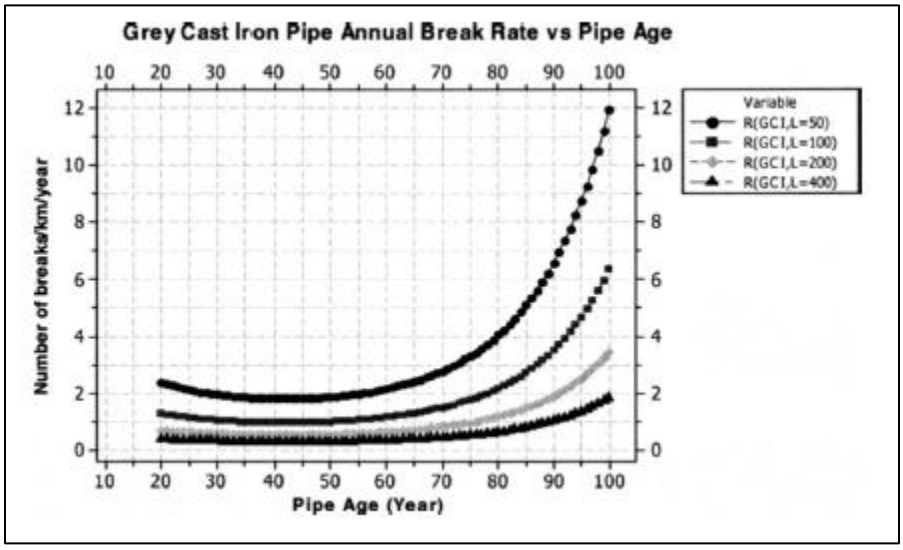

Figure 12. Break rate vs. age for cast iron pipes 100 m long of varying diameters (Wang et al., 2009).

Limitations of the Wang et al. models (2009) in relation to the Ste-Foy case study include the inability to predict future breaks and the lack of consideration of past repairs, cathodic protection, and soil conditions in the model. In relation to the Barton Springs segment of the Edwards Aquifer the Wang et al. models (2009) are limited by their single application to a small municipality. To apply these regression models to the water main

distribution data to the City of Austin, this study assumes they may be replicated in alternative locations such that climatic and geologic conditions do not change the results.

2.3 Groundwater Models of the BSEA

The uncertainty of groundwater parameters, in addition to the complexity of groundwater systems, present challenges for those charged with managing such resources to meet ecological needs. For this reason, resource managers often use groundwater models to predict the availability of groundwater in response to aquifer stresses, such as pumping withdrawals and drought conditions. Groundwater models are a simplified representation of dynamic natural aquifer systems and must be calibrated by the user with validated field data. Due to the fact individual models have unique sets of limitations, it is important to maintain this awareness when generating model runs and interpreting data.

Multiple versions of digital groundwater flow models have been created for the Barton Springs segment of the Edwards Aquifer over the past 30 years (Slade et al., 1985; Barrett and Charbeneau, 1997; Scanlon et al., 2001; Scanlon et al., 2003; Smith and Hunt, 2004; Lindgren et al., 2004; Lindgren, 2006; Painter et al., 2007; Passarello, 2011; Hutchinson and Hill, 2011). Each model addresses water quantity or quality predictions in the BSEA with a different set of parameters or calibration factors. This project uses Passarello's model (2011), adapted from Scanlon et al.'s 2001 Groundwater Availability Model (GAM) for urban recharge considerations, to maximize well withdrawals for the BSEA to meet attainable pumpage rates without reaching drought status according to the BSEA's Drought Trigger Methodology.

This project uses the BS GAM model framework developed by Scanlon et al. (2001), as it was the first model for Barton Springs segment of the Edwards Aquifer approved by the State of Texas and utilizes commercially available, USGS-developed MODFLOW-96 code (Harbaugh and McDonald, 1996). Varied criticisms of the 2001 BS GAM led to the model's recalibration for drought-of-record conditions (Smith and Hunt, 2004; Hutchinson and Hill, 2011), the development of a dual-conductivity model for the BSEA with GAM as a baseline (Painter et al., 2007), and the integration of urban recharge considerations (Passarello, 2011). Using the most accurate recharge interpretation file

(Natural + Artificial Recharge) developed by Passarello (2011) to measure discharge within the BS GAM, this project integrates stochastic pipe break predictions and optimization techniques to predict sustainable withdrawal rates for all wells within the BSEA.

2.3.1 MODFLOW Code

The United States Geological Survey (USGS) created MODFLOW, Modular Three-Dimensional Finite Difference Groundwater Flow Model, the present-day standard computer modeling software to simulate flow through aquifer systems. MODFLOW source code, primarily written in FORTRAN, is free to the public. McDonald and Harbaugh released the first version of MODFLOW in 1983, which has since undergone several updates in 1988, 1996, 2000, and 2005. The most recent version as of this study is MODFLOW-2005. Several processes and packages have been added to MODFLOW for groundwater management than can be used with MODFLOW-2000. This study uses the Groundwater Management package, known as MODFLOW-GWM., for optimization of well withdrawals. As Scanlon et al. (2001) created the original BS GAM with MODFLOW-96, and the GWM optimization process is only compatible with the 2000 version and beyond, this study uses the MF96TO2K conversion package to convert the files to a MODFLOW-2000 model (Ahfeld et al., 2005).

The MODFLOW code used for the model simulations employs the partial differential equation for three-dimensional flow in a heterogeneous and anisotropic unconfined or confined aquifer, which incorporates Darcy's Law (McDonald and Harbaugh, 1988):

$$\frac{\partial}{\partial x}\left(K_{xx}\frac{\partial h}{\partial x}\right)+\frac{\partial}{\partial y}\left(K_{yy}\frac{\partial h}{\partial y}\right)+\frac{\partial}{\partial x}\left(K_{zz}\frac{\partial h}{\partial z}\right)-W=S_s\frac{\partial h}{\partial t} \quad (3)$$

where

K_{xx}, K_{yy}, K_{zz} = hydraulic conductivities along the x, y, and z coordinate axes, assumed to be parallel to the major axes of hydraulic conductivities [Lt^{-1}]

H = potentiometric head [L]

W = volumetric flux per unit volume representing sources and/or sinks of water [t^{-1}]

S_s = specific storage of the porous medium [L^{-1}]

t = time [t]

With the assumption fluid density is constant, a groundwater flow system representation includes Equation 3 with the combination of initial head and boundary conditions. The equation of linear systems created by the flow system requires a numerical solution, such as the finite difference method, which is used in MODFLOW code. It is important to note that Darcy's Law does not apply to turbulent flow, which is often present in the conduits of karstic aquifers and near wells, and instead serves as an overall simplification of the BSEA. Scanlon and others recognize this limitation and note it is not critical for water resources management, particularly since the 2001 model simulations effectively predicted variations in spring flow and monitoring well water levels over time.

2.3.2 The MODFLOW-96 Groundwater Availability Model for the BSEA

The primary framework used for this research, the 2001 GAM by Scanlon et al. is a two-dimensional, numerical finite-difference groundwater flow model for the BSEA. The authors created the BS GAM for the BSEACD to evaluate groundwater availability of Barton Springs and predict spring flows and water levels from 2001-2050 "in response to increased pumpage and droughts" (Scanlon et al., 2001). In addition, they developed the 2001 BS GAM to more accurately predict groundwater availability in Barton Springs than

two models previously created for the aquifer (Slade et al., 1985; Barrett and Charbeneau, 1996). Slade et al. (1985) developed a two-dimensional, finite-difference groundwater flow model for the U.S. Geological Survey (USGS) in response to concerns of urban development. Scanlon et al. (2001) criticized this model for its outdated code (Trescott et al., 1976), coarse grid size (a minimum of 1,500 feet), and short simulation for transient flow (5 months). In response, they used a minimum grid size of 500 feet and a transient flow simulation of 10 years (1989-1998). Barrett and Charbeneau (1996) developed lumped parameters to model the BSEA parsimoniously, citing fewer parameters and calibrations. The lumped parameter model represented the BSEA with only five cells, one for each of the contributing watersheds. In each cell, Barrett and Charbeneau (1996) modeled conditions using a single well. While this model effectively represented water levels and nitrogen concentrations in the BSEA, Scanlon et al. (2001) noted the model's coarse nature did not accurately represent the impact of local pumping on spring discharge and water levels.

The 2001 BS GAM comprises a single layer, a 120 row by 120 column grid, with 14,400 total cells. The model's active cells overlay the area of the BSEA and amount to 7,043. The cells are rectangular in size with a length of 1,000 feet and a width of 500 feet. The authors rotated the model 45 degrees from the horizontal to align the rows parallel to the strike of the Edward's Aquifer. The boundaries of the BS GAM include the Colorado River (Lady Bird Lake) to the north, the groundwater divide along Onion Creek to the south, which separates the two segments of the Edwards Aquifer (LGB-Guyton and Associates, 1958), the *"bad-water"* line to the east, which signifies the zone where total dissolved solids exceed 1,000 mg/L, and the no-flow boundary of the Mount Bonnell fault to the west (Senger and Kreitler, 1984; Scanlon et al., 2001).

The BS GAM utilizes parameters such as initial head values, elevations for the top and bottom of the layer, and hydraulic conductivity. The authors ran three simulations with the BS GAM: steady state, transient, and predictive. Initial head values were equivalent to the top elevation of the aquifer for all simulations. In addition to head values and hydraulic conductivity, the transient model also used specific storage and specific yield as model parameters.

To determine the losing streams recharge for the BS GAM, which Slade et al. (1985) noted to be approximately 85% of the total recharge in the BSEA, Scanlon et al. (2001) used data from pumping stations. They then set diffuse recharge to be the remaining 15%, which they estimated as a percentage of the total recharge. The 2001 model assigns pumping to active cells within the grid. The BSEACD estimated unreported pumping for the model.

The steady state simulation, which Scanlon et al. (2001) created to evaluate the spatial distribution of hydraulic conductivity, integrates average recharge for a twenty year period (1979-1998) and pumpage values from 1989. For the transient BS GAM simulation, they used monthly recharge and pumpage values for a ten-year period (1989-1998). They chose values from this time period due to the fluctuation of high and low water levels. The predictive simulation initially used pumpage data from 2000 and linearly interpolated future pumpage estimates for 2001 through 2050. In addition, the authors estimated recharge for the simulation in an attempt to match the 1950-1956 drought of record.

Overall, Scanlon et al. (2001) noted generally good agreements for the simulated and measured hydraulic head drops and discharges in each simulation. For the steady state model, they found the root mean square (RMS) error to be 24 ft (7.3 m), approximately 7% of the total head drop cross the study area. The RMS error was 12 cfs (0.34 cms) for the transient simulation, approximately 11% of the discharge fluctuations for the simulated time period. Limitations to the 2001 BS GAM include, but are not limited to: the circular reference of recharge and discharge, lack of spatial distribution in recharge, the simulation of the "bad-water" zone as a finite line, and the lack of hydrologic connection between the Upper Trinity Aquifer and the Edwards Aquifer. Although the authors note additional limitations, they are not directly related to this study.

2.3.3 BS GAM Adaptions for Artificial Recharge

Using the 2001 BS GAM, Passarello (2011) integrated new recharge input files with spatial and temporal resolution. Passarello's updates to the recharge files not only includes these resolutions, it is also the first BSEA model to estimate anthropogenic, or artificial, recharge and disconnect the circular connection between discharge and recharge.

Anthropogenic, or artificial recharge, is the presence of hydrologic inputs due to human activity that would not exist in the natural system and may include sources such as municipal water networks, injection wells, storm water catchments, irrigation return flows, etc. (Sharp, 2010). Using extensive data sets such as precipitation, land use, pumpage, and pipe network data, along with GIS spatial analysis techniques, Passarello calculated anthropogenic recharge to account for <1-52% of the total recharge in the BSEA, depending on natural hydrologic conditions, and averages 4% of total recharge overall.

For new recharge inputs, Passarello considered four types of recharge: diffuse, indirect, stream, and irrigation return flow. The total recharge for the input files is the sum of the four types. Diffuse recharge is the direct infiltration of precipitation; indirect recharge includes that from anthropogenic sources such as water distribution and sewer lines, septic tanks, and storm water systems, such as sewers and holding ponds. Passarello found the recharge interpretation file with the greatest agreement to be the Altered Natural + Artificial scenario that includes an infiltration rate of 6% from a study by Barrett and Charbeneau (1996) rather than the Natural + Artificial scenario that assumes 21 and 32% for impervious surfaces and land cover, respectively (Wiles and Sharp, 2008; Hauwert, 2009). For Passarello's model, and thus the Altered Natural + Artificial recharge file for this project's model, indirect recharge only includes that from water distribution and wastewater networks. Irrigation return flow includes recharge that does not infiltrate as a result of overwatering urban landscapes, such as lawns, parks, golf courses, etc. Finally, Passarello included stream recharge from the six losing streams in the BSEA.

Passarello's spatial and temporal changes to recharge inputs for the BS GAM model prove valuable for groundwater management of the BSEA. The 2011 model displayed good agreement between simulated and measured discharge and water-level elevations with a RMS error of 17.7 cfs (0.5 m^3/sec) and 34 feet (10.5 meters), respectively. Although leaky utility lines comprised the highest overall percentage of Passarello's anthropogenic recharge findings, the model also revealed that when anthropogenic recharge was at its greatest percentage of total recharge, irrigation return flow provided the greatest contribution. Ultimately, Passarello found anthropogenic recharge contributions

comparable to those of a mid-sized watershed, thus proving a "critical source for buffering seasonal fluctuations, particularly during low flow periods" (2011).

2.3.4 Additional Updates to the BS GAM

Updates to the 2001 BS GAM occurred both prior to and after Passarello's recharge contributions. The prior updates were not included in Passarello's 2011 model. Smith and Hunt recalibrated the BS GAM in 2004 to more accurately reflect drought conditions, as the 2001 model's calibrations were for a more hydrologically wet time period than the 1950's drought-of-record. This model not only demonstrated a better match between simulated and measured spring-flows and water-levels than the 1950's drought than the 2001 BS GAM, it also predicted significantly lower water levels to occur as a result of projected pumping rates than the previous model.

In 2011, Hutchinson and Hill recalibrated the original BS GAM for drought conditions after a request from Groundwater Management Area 10. This request specified model runs to produce streamflows at Barton Springs of 11, 9, 7, 5, and 3 cfs under drought-of-record conditions, which were not provided in the original BS GAM's estimated minimum flows of 11 cfs under drought-of-record-condition. This model, known as the Alternative Barton Springs Groundwater Availability model, includes a calibration time period from 1943 to 2004 and was emphasized for the drought-of-record years 1950-1956. The authors note the narrow scope of this model limits its applications.

The second update to the 2001 BS GAM was that of a dual-conductivity model, created by Painter et al. in 2007. The dual-conductivity model integrates the original 2001 model into MODFLOW-DCM with a conduit/matrix groundwater flow system to simulate a wide range of hydrologic situations and simulate turbulent and laminar flow conditions of a karst aquifer (Lindgren et al., 2009). Painter et al. (2007) developed MODFLOW-DCM version 2.0 to incorporate a solver capable of solving highly non-linear systems accompanying the model's complex conduit/matrix groundwater flows. Passarello notes that although Painter et al. (2007) distributed recharge with a different method, with recalculations they can be integrated with the DCM model.

2.4 Optimization using MODFLOW Groundwater Management (GWM)

Previous models for the BSEA provide optimal levels of spring flow discharge at Barton Springs, yet none have optimized pumpage rates of the aquifer's wells through modeling programs. Through a MODFLOW process known as Groundwater Management, or GWM, (Ahfeld et al., 2005), various management concerns, such as economics and water levels, can be maximized or minimized with unique set of equations. The GWM process generates an output response-matrix to solve linear, nonlinear, and mixed binary management equations to achieve the desired optimized outcome on MODFLOW-2000 or MODFLOW-2005. This project uses GWM-2000 with Passarello's 2011 model to optimize well withdrawals in the BSEA. As the model used for this project is originally in MODFLOW-96 format, the author converted the model to MODFLOW-2000 using the conversion package MF96TO2K.

2.4.1 GWM Formulation

A GWM-2000 groundwater management formulation consists of a set of decision variables, an objective function, and a set of constraints. MODFLOW supports decision variables that include flow-rate, external, and binary variables. The purpose of the objective function is to maximize or minimize the desired output, and can include one or any combination of the decision variables. Finally, GWM-2000 can include four types of constraints: decision-variable, linear summation, hydraulic head, and streamflow. The solution through the response matrix in GWM requires the objective function and set of constraints to be expressed as functions of the decision variables. GWM then uses simplex, as well as branch and bound, algorithms to solve the specified groundwater management formulation. The algorithms are coded into GWM-2000 using FORTRAN-90 computer language.

2.4.2 Decision Variables

The decision variables for the groundwater management formulation are the determined solution to the designed problem, such as pumpage rates for the designated wells within the BSEA. Decision variables can be considered as "controls" (Ahfeld et al.,

2005) and include flow-rate, external, and binary variables. Flow-rate variables include withdrawal or injection rates of wells, external decision variables include external sources or sinks to the modeled system that do not affect the state variables of the simulated system such as heads, streamflow, etc. Binary decision variables define the status of the previous two variables by designating their use as a 1 or 0. Ahfeld et al. (2005) note binary variables may complicate computations within GWM-2000 and should be used with caution. Both flow-rate and external decision variables can be simulated over multiple stress periods.

2.4.3 Objective Function

The objective function of the groundwater management formulation maximizes or minimizes, i.e. optimizes, the weighted sum of set combination of decision variables. (Ahfeld et al., 2005). Each GWM-2000 process includes one objective function. The objective function may include coefficients to express an outcome in total economic costs, represented in general form by Equation 4:

Maximize or minimize

$$\sum_{n=1}^{N} \beta_n Qw_n T_{Qw_n} + \sum_{m=1}^{M} \gamma_m Ex_m T_{Ex_m} + \sum_{l=1}^{L} \kappa_l I_l \quad (4)$$

subject to constraints

where

β_n = the cost or benefit per unit volume of water withdrawn or injected at well site *n*;

γ_m = the cost or benefit per unit volume of water imported or exported at external site *m*;

κ_l = the unit cost or benefit associated with the binary variable I_l;

T_{Qwn} = the total duration of flow at well site *n*;

$T_{Ex}m$ = the total duration of flow at external site *m*;

N,M,L = the total number of flow-rate, external, and binary decision variables, respectively

2.4.4 Constraints

The four types of constraints supported by GWM-2000 are lumped into two categories: two types that do not require response coefficients and two types that do require the generation of response coefficients. Constraints on decision variables, such as upper or lower bounds on flow-rates or external variables, and linear summation constraints, such as the total number of active wells or net system stress, are in the category of constraints that do not require the generation of response coefficients in the response matrix. Hydraulic head and streamflow constraints are the two types of constraints that do require response coefficients. Hydraulic head constraints can include absolute lower or upper bounds, drawdown constraints, head difference between two locations, and the gradient in head between two locations (Ahfeld et al., 2005). The two types of streamflow constraints include absolute lower or upper bounds on streamflow and streamflow depletion.

2.4.5 GWM Solution

The type of solution to the groundwater management formulation depends on whether the required programming involved is linear, nonlinear, or binary. In general, the Response Matrix Solution package of MODFLOW-GWM uses three different approaches for each unique solution. While a linear program formulation includes both a linear objective function and only linear constraints, a nonlinear formulation includes a nonlinear objective function and one or more nonlinear constraints. Binary solutions apply to formulations that include binary variables.

2.5 Justification of Research

As current groundwater models for the BSEA are deterministic in nature, particularly the BS GAM, this research works toward developing a stochastic model to provide predictions of the contribution of urban, or artificial, recharge from water main breaks within the City of Austin, Texas. Additionally, this research develops the first MODFLOW-GWM package to be used in conjunction with both deterministic and stochastic model simulations of the BS GAM. Drought trigger constraints, specifically head levels at the Lovelady Monitoring well, are using within the GWM package to

optimize well pumpage. Both modeling practices created in this project serve to aid stakeholder-management conversation, policy development, and future research.

Chapter 3: Methodology

The purpose of this project is to develop a stochastic method to evaluate artificial recharge contributions in the Barton Springs segment of the Edwards Aquifer and assess the resiliency and reliability of the aquifer in response to future demand. As neither a stochastic model nor a MODFLOW-GWM package has been developed for the BS GAM previously, this research works toward developing both modeling practices for a more innovative groundwater management process and subsequent research with a Monte Carlo and Bayesian analyses. For insight on the bounds of uncertainty for future stochastic results, this research analyzes maximum, mean, and minimum recharge scenarios. As a final application, the author developed a GWM package for various scenarios of the original BS GAM model (Scanlon et al., 2001; Passarello, 2011) to maximize optimal withdrawals according to drought trigger constraints set by the BSEACD. Figure 13 provides a flow chart for the process of methods described in this chapter.

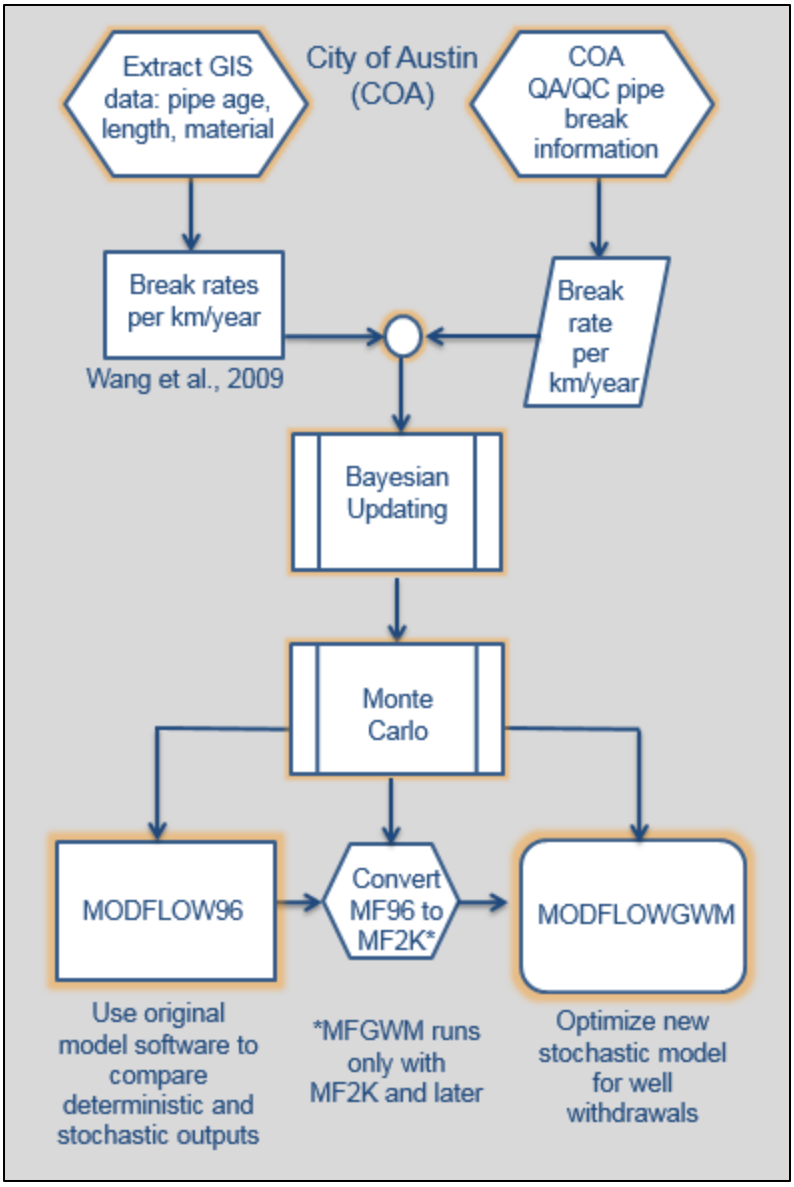

Figure 13. Methods flow chart.

3.1 Software

Stochastic model runs employ the use of MODFLOW96, the modeling software used for the initial model runs of both Scanlon et al. (2001) and Passarello (2011). MODFLOW-GWM requires the use of MODFLOW-2000 or -2005 format. As the BS GAM files were created with MODFLOW-96, the author ran a conversion software package to transform the files to the 2000 format. The author manually updated the

Horizontal Flow Barrier (HFB) file to 2000 format, which the MODFLOW-2000 User Documentation indicated as necessary. A comparison of heads between the two model runs in Groundwater Vistas 6 produced differences no greater than 10^{-4} feet, a value low enough to consider the conversion acceptable.

3.2 Stochastic Recharge

The objective of this section is to determine stochastic recharge rates for the BS GAM utilizing water distribution risk models and compare the results with the updated recharge rates employed by Passarello (2011) for the January 1, 1999 to December 31, 2008 time period. Model outputs are compared to Passarello's Altered Natural + Artificial recharge interpretation, the closest model simulation to measured discharge at Barton Springs for the 1999-2008 time period (2011). The software used to calculate the range of recharge values includes ArcGIS 10.1.3, Microsoft Excel, MODFLOW-96, and MODFLOW-GWM.

Passarello (2011) modified recharge inputs to the original BS GAM (Scanlon et al., 2001) through land use considerations, artificial and urban recharge, and updated flow loss surveys. This project only modifies the artificial recharge from water distribution sources in the recharge zone of the Barton Springs segment of the Edwards Aquifer. The reader is referred to Passarello (2011) for methodology on the recharge modifications to the original BS GAM.

3.2.1 ArcGIS Processing

The objective of using ArcGIS 10.3.1 for this project is to obtain water distribution characteristics within the BS GAM geographical region for statistical processing to determine stochastic recharge rates. Additionally, data stored in the BS GAM shapefile includes unique identifiers known as "HydroIDs", which MODFLOW reads to code input data to individual BS GAM cells. The data required by ArcGIS processing includes total pipe length by BS GAM cell by year, water distribution data according to pipe material (cast iron, ductile iron, PVC) for the model boundaries, and the primary (highest count) pipe material by BS GAM cell.

The City of Austin provided an updated water distribution shapefile for the project and faculty at the University of Texas at Austin provided the BS GAM shapefile. All files retrieved are in the required spatial reference (NAD 1983 State Plane Texas Central FIPS 4203 Feet). The first step in ArcGIS was to obtain water distribution data for the BS GAM area using the *Clip* tool. This dataset was then exported as a separate shapefile for further use. Next, pipe data was linked to MODFLOW grid cells, identified by unique HydroIDs, using the *Join* tool. As multiples of HydroIDs existed in the attribute table, the *Dissolve* tool combined data according to the HydroID field and enabled to the total length of pipe per BS GAM cell (HydroID) to be obtained.

To retrieve total water main lengths in existence each year from 1999 – 2009, queries were employed. The select pipe data for each year was then exported as individual shapefiles. For this step, the author assumed the "Date Proposed" field to be the first year of existence for the corresponding pipe and files with "0" as the proposed date to have been added prior to 1999, as recommended by the City of Austin (Personal Communication, 2016). As an example, the 1999 pipe data shapefile contains all years prior to 1999, including the "0" files.

Similarly, queries were used to obtain pipe data according to pipe material. These data sets included all years within the clipped shapefile prior to it being joined to HydroIDs. This data was exported to Microsoft Excel for statistical processing. To find the primary pipe type by BS GAM cell (HydroID), queries were performed for the 1999 and 2009 pipe shapefiles to extract total pipe length by HydroID for each pipe material type, including cast iron (CI), ductile iron (DI), and PVC. Additional pipe materials exist within the data set and were summed and designated as "OTHER" for future coding purposes. Each query by pipe type was exported as a unique shapefile and ultimately joined to the original BS GAM shapefile to obtain a shapefile that contained total length for each pipe material per HydroID. After exporting the table from this shapefile to Excel, a simple programming statement coded a pipe "type" according to the pipe type with the greatest length per HydroID. For simplicity, the 2009 data codes are used in the stochastic analysis.

3.2.2 Monte Carlo Analysis

To obtain a range of recharge inputs for a stochastic analysis, this project uses a Monte Carlo simulation with pipe break prediction models for gray cast iron, ductile iron (without lining), and PVC pipes (Wang et al., 2009). While many types of pipe break modeling exist, this project utilizes regression models developed by Wang et al. (2009) due to the available water distribution data provided by the City of Austin and reproducible nature of the models. A simplifying assumption in the application of these models is to the overlap of environmental conditions, such as climate, soil type, and geology, from Wang et al.'s study (2009) in Ste-Foy, Ontario to Austin, TX water distribution pipe data

The Monte Carlo analysis uses statistical parameters (i.e. mean and standard deviation) from each of the cast iron, ductile iron, and PVC data sets to obtain a series of random variables as the output, which, in the case of the Wang et al. (2009) regression models is break rate per kilometer per year. The regression models developed by Wang et al. (2009) are as follows:

Gray Cast Iron

$$Log_{10}R = 4.85 - 0.0206A + 0.000245A^2 + 0.00281S - 0.905Log_{10}L - 1.40Log_{10}S \quad (5)$$

where

R = annual break rate [number of breaks/km/year];
A = water main age at year 2001 [year];
S = water main size, diameter [mm];
L = water main length in GIS database [m];

Ductile Iron (lined)

$$Log_{10}R = 3.36 - 0.000150L \times A - 1.11Log_{10}L - 0.646Log_{10}A - 0.254Log_{10}S \quad (6)$$

PVC

$$Log_{10}R = 2.69 - 0.898Log_{10}L - 0.745Log_{10}A \quad (7)$$

For each pipe type, 10,000 break rates are generated. From this data, minimum, maximum, and mean break rates per pipe type provide bounds of uncertainty and expected averages for recharge interpretations.

3.2.3 Bayesian Analysis

Uncertainty in the Wang et al. models (2009) is narrowed for this project using a Bayesian analysis technique (Bayes, 1763), which updates prior information (i.e. Wang et al. model distributions (2009) with observed data. For this project, observed break rate information is calculated through quality assured/quality controlled (QA/QC) water distribution break work orders (City of Austin, 2016; Equation 8). The Bayesian analysis is performed with pipe material average break rates from the regression models (Wang et al., 2009), the respective probabilities of pipe occurring by material within the BS GAM, and the observed break rate data to yield new probabilities of break averages by pipe material (Equation 9). Updated mean break rate probabilities by pipe material determine the distribution of breaks across model cells in the BS GAM for the new recharge interpretations.

$$R_{obs} = \frac{\sum WB}{\sum WD_L} \quad (8)$$

where

R_{obs} = observed break rate [per km/year];
WB = observed annual breaks;
WD_L = total annual water distribution system length [km]

$$P(\Theta = \theta_i|\varepsilon) = \frac{P(\varepsilon|\Theta=\theta_i)P(\Theta=\theta_i)}{\sum_i^n P(\varepsilon|\Theta=\theta_i)P(\Theta=\theta_i)} \quad (9)$$

where

P = probability;

θ_i = distribution parameter; i.e. pipe break mean by material [per km/yr];

Θ = modeled random variable for θ_i [breaks/km/yr];

ε = observed information [breaks/km/yr]

3.2.4 Pipe Break Rates to Recharge Conversion

As the BS GAM requires a monthly leakage value (ft^3) for a recharge input, the break rate (per km/yr) is converted to a monthly flow loss per kilometer of pipe (Equation 10):

$$WW_m = \frac{R \times L_{Avg}}{12} \quad (10)$$

where

WW_m = monthly flow loss per kilometer of pipe [ft^3];

R = annual break rate [number of breaks/km/year];

L_{Avg} = average flow loss per break [ft^3]

The average flow loss per break is calculated using QA/QC City of Austin pipe break work orders from 2009-2015, which contains the estimated flow loss per break of water distribution mains (City of Austin, 2016). While some pipe break information includes pipe characteristics, such as material type and size, not enough is available to perform further statistical analyses, such as city-specific regression curves.

For this scope of this project, only the minimum, maximum, and mean pipe break rates are used to assess the average values and bounds of uncertainty for the stochastic analysis. Once monthly flow loss values (per km) and their probabilities of occurring according to pipe material are calculated using Monte Carlo and Bayesian analysis, respectively, these values are multiplied by the total pipe length (km) per BS GAM cell to represent the total monthly recharge from the City of Austin's water distribution system.

This updated recharge is added to the remaining recharge values (irrigation return flow, wastewater leakage, precipitation, and streamflow) determined by Passarello (2011) to obtain the final recharge file. To write this file in MODFLOW format, recharge values (length per time) are created for each HydroID at each time step and exported as a text file.

3.3 Optimization

The purpose of this section is to describe the methodology for MODFLOW-GWM. Upon completion of the stochastic analysis tests in MODFLOW96 a second set of tests are performed using MODFLOW-GWM to assess the optimal amount of withdrawal for the BSEA using the Lovelady Monitoring Well as a head constraint. MODFLOW-GWM requires file inputs for an optimization function, decision variables, constraints, and a solution algorithm and applies these files to a MODFLOW scenario, known as the "background" test. MODFLOW-GWM tests are run using Passarello's Altered Natural + Artificial Scenario and the associated stochastic scenarios as background MODFLOW models (2011). Alternative tests using Passarello's Natural + Artificial Scenario (2011), which simulates 160% greater recharge than the Altered scenario due to increase infiltration rates, is run in MODFLOW-GWM for comparison.

3.3.1 Optimization Function and Decision Variables

In addition to updating the recharge input file for the original BS GAM model (Scanlon et al., 2001), Passarello updated the well file to provide a more discretized pumping scenario throughout the aquifer. Scanlon and others simulated well withdrawals by applying an averaged pumping rate to each active cell in the model, other than the cells used to simulate Barton and Cold Springs, for a total of 7,037 well cells. Passarello provided updated pump data from a report by Hunt et al. (2006) to discretize pumping by approximate monthly percentages over 90 well cells (Appendix B). The decision variables used for this project are flow rate decision variables and include each of the 90 simulated wells in the updated BS GAM model (Passarello, 2011). The objective function will maximize the total withdrawals from each decision variable with equal benefit, or weight, assigned to each well (Equation 11).

Maximize

$$\sum_{n=1}^{N} 1.0 Q_{w_n} T_{Qw_n} \quad (11)$$

subject to head constraints (Equation 13)

where

Qw_n = the total withdrawal at well site *n* for duration $T_{Qwn;}$ [ft^3];

T_{Qwn} = the total duration of flow at well site *n*; [t]

N = the total number of flow-rate decision variables

Due to data processing limitations, at most, 90 withdrawals are optimized on a biennial scale and summed to achieve total annual withdrawals. It should be noted that flow rates designated by the original model's well data file are unique from the decision variables (Ahfeld et al., 2005). While, for this project, the decision variables reference the same well cells as the original model's data file (wel.dat), the optimization withdrawal values serve only as a reference point for optimization and assume an initial value of zero. If the original model's well file were to be included in the GWM optimization, a solution would be obtained using decision variable wells that would need to be pumping simultaneously with the background wel.dat file.

From the 90 flow-rate decision variables, Well 42 (Row 66, Column 43) carries the least weight of all wells at 0.002% of total withdrawals, while Well 22 (Row 104, Column 23) carries the greatest weight at 10.55% (Appendix B). The flow-rate decision variables represent the minimum and maximum monthly withdrawals (Equation 12). The minimum withdrawals will always have a bound of zero, while the maximum withdrawals vary for analyses.

$$Qw_n{}^{l} \leq Qw_n \leq Qw_n{}^{u} \quad (12)$$

where

$Qw_n{}^{l}$= the lower bound on the flow-rate decision variable, *n* [ft^3];

Qw_n= the volume of water withdrawn at well site *n*, [ft^3];

Qw_u^u= the upper bound on the flow-rate decision variable, n [ft^3];

Maximum withdrawal rates were obtained from the most recent BSEACD report regarding wells and pumping in the Barton Springs segment of the Edwards Aquifer (Hunt et al., 2006; Figure 14). To maximize the amount withdrawn for the GWM model, decision variables included the permitted value from Fiscal Year 2006 (FY2006), the highest amount permitted, in addition to the estimated withdrawals from exempt (non-permitted) users. Of 94 permittees in 2006, permitted pumpage for the BSEACD was approximately 2.5 billion gallons (2,469,469,937 gallons), while metered pumpage was approximately 2.1 billion gallons (2,076,742,335 gallons; Appendix A). The BSEACD estimates exempt pumpage, such as domestic and agricultural well users, to be 11% of annual permitted pumpage, resulting in an estimation of 228,441,657 gallons for FY2006. For the GWM model, FY2006 permitted and exempt pumpage resulted in an annual withdrawal of 2,698,359,102 gallons, or approximately 11.4 cfs distributed among the 90 decision variables (Hunt et al., 2006).

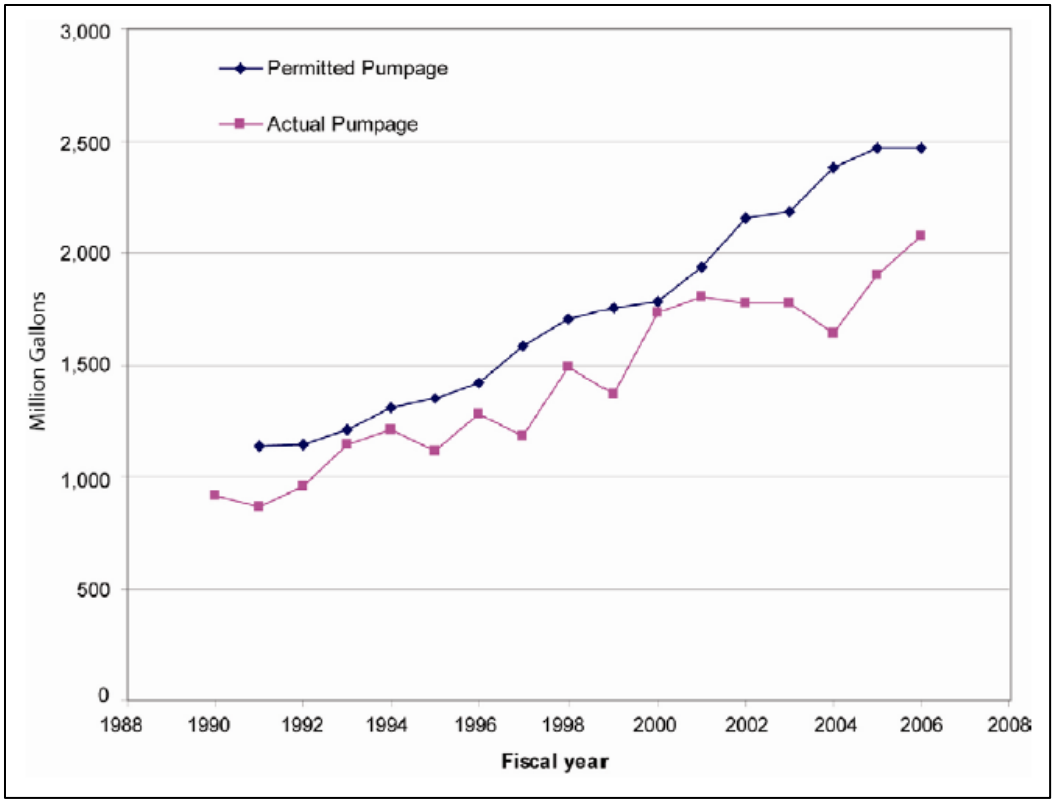

Figure 14. Permitted and actual (metered) pumpage for the BSEACD; exempt wells not included in figure (Hunt et al., 2006).

3.3.2 Constraints

The optimization function for this project is subject to a hydraulic head constraint, which simulates the Lovelady Monitoring Well, one of two drought triggers for the BSEACD. The BSEACD implements conservation measures and issues an "Alarm Drought" status when the head level at the Lovelady Monitoring Well falls below 478.4 feet above mean sea level. Additionally, the DTM Lovelady Monitoring Well levels "Critical Drought", "Exceptional Drought", and "Emergency Response" scenarios are 462.7, 457.1, and 453.4 feet, respectively. These values serve as a lower bounds for the head constraint for various simulations in the optimization process (Equation 13).

$$h_{i,j,k,t} \geq h^{l}{}_{i,j,k,t} \quad (13)$$

where

$h_{i,j,k,t}$ = the head at location *i, j, k* at the end of stress period *t* [ft];

$h^{l}{}_{i,j,k,t}$ = the lower bound on head at location *i, j, k* at the end of stress period *t* [ft];

Typically, groundwater management formulations would include streamflow constraints on the original models streamflow (STR1) file. In this case, the second drought trigger in the BSEACD, discharge levels at Barton Springs, would serve as the lower streamflow constraint, represented in the STREAMCON file. However, since drain (DRN) files represent the discharges at both Barton and Cold Springs, this constraint is unable to be utilized.

3.3.3. Solution Algorithm

Ultimately, the complete optimization formulation for this project will be:

Maximize

$$\sum_{n=1}^{N} 1.0 Q_{w_n} T_{Qw_n} \quad (11)$$

subject to

$$0 \leq Qw_n \leq Qw_n{}^{u} \quad (12)$$

$$h_{i,j,k,t} \geq h^{l}{}_{i,j,k,t} \quad (13)$$

where

Qw_n = the total withdrawal at well site *n* for duration $T_{Qwn;}$ [ft^3];

T_{Qwn} = the total duration of flow at well site *n*; [t]

N = the total number of flow-rate decision variables;

$Qw_u{}^{u}$ = the upper bound on the flow-rate decision variable, *n* [ft^3];

$h_{i,j,k,t}$ = the head at location *i, j, k* at the end of stress period *t* [ft];

$h^{l}_{i,j,k,t}$ = the lower bound on head at location *i, j, k* at the end of stress period *t* [ft];

As the exact mathematically relationship between aquifer withdrawals and the designated constraints is nonlinear (variable transmissivity), the solution file to the groundwater management formulation calls the sequential linear programming (SLP) approach as its designated solver process for the Response Matrix Solution package. However, if initial tests from the SLP approach prove similar to the linear programming (LP) solution, which requires less space and time per simulation, the LP solution file may be applied to subsequent simulations (P. Barlow, personal communication, 2016).

3.4 GWM-2000 Scenarios

The pumping optimization for this project involves multiple scenarios. The author used Passarello's well file, altwel.dat, to apply pumping percentages to each of the 90 well cells across the BSEA for the minimum and maximum pumping rates for the GWM input file. For optimization purposes, the minimum pumping rate for each well is zero cfs, while the maximum overall pumping rates correspond to each wells percentage of the highest monthly pumping value from Hunt and other's 2006 report. Initial simulations are run to gain insight on the sensitivity of head closure criterion (HCLOSE) used to solve the finite difference equations in the strongly implicit procedure (SIP) package of the background BS GAM model (Table 2). Additional model simulations will include the application of GWM to each of Passarello's Altered Natural + Artificial and Natural + Artificial recharge scenarios (2011) to gain insight on the impacts of recharge to optimal withdrawals (Table 2). Using DTM Lovelady Monitoring Well levels, decreasing head constraint files are applied for each recharge scenario when no optimal solution is found.

Table 2. Summary of GWM-2000 simulations.

Name of Scenarios	Description	Background Recharge File	Number of Simulations	Number of Objective Wells per Simulation
Sensitivity Analysis	Observe % of withdrawal objective met by altering Head Closure Criterion (HCLOSE) using linear programming (LP); run a simulation with sequential linear programming (SLP) for comparison	Natural + Artificial (N+A), (Passarello, 2011)	3 LP 1 SLP	90
Drought Trigger Methodology (DTM)	Observe % of withdrawal objective met by altering head constraints on the Lovelady Monitoring Well according to DTM levels	Altered N+A, N+A (Passarello, 2011)	4 of each recharge file	90
Performance Criteria	Observe % of objective met, reliability, and resilience for tests with greater discretization	Altered N+A, N+A (Passarello, 2011)	1 of each recharge file	450

3.5 Performance Criteria

To assess groundwater withdrawal management within the BSEA, BSEACD allocated withdrawal rates, or demand, and the maximum rates set by GWM for the same time period will be evaluated with a set of performance criteria. The performance criteria of resilience and reliability will characterize trends in groundwater management of Barton Springs and to provide valuable information to stakeholders. For a given time period, a deficit occurs when allocated groundwater withdrawals exceed maximum rates (Teasley, 2009) (Equation 14).

$$D_i^t = \begin{cases} 0 & if\ X_i^t = Demand_i^t \\ Demand_i^t - X_i^t & if\ X_i^t < Demand_i^t \end{cases} \quad (14)$$

where

D_i^t = deficit [ft^3];

X_i^t = the delivery of water to user *i,* at the end of stress period *t* [ft^3];

$Demand_i^t$ = the demand of water by user *i,* at the end of stress period *t* [ft^3]

For each time period, the performance criterion reliability represents the probability the maximum optimal withdrawals meet the given demand set by the BSEACD and thus, no deficit occurs (Klemes et al., 1981; Hashimoto et al., 1982; McMahon et al., 2006) (Equation 15).

$$Reliability_i = \frac{n_{D_i^t=0}}{N} \tag{15}$$

where

$n_{D_i^t=0}$ = the number of zero deficit time periods for user *i* for all time period lengths *t* in the simulation;

N = the total number of time periods of length *t* in the simulation

Resilience is the criterion used to assess the response of varying stress conditions and user demand. A system is considered resilient if it experiences a recovery time period, i.e. demand is achieved, following a period of failure, or deficit (Hashimoto et al., 1982) (Equation 16).

$$Resilience_i = \frac{\#\ of\ times\ D_i^t=0\ follows\ D_i^t>0}{n_{D_i^t>0}} \tag{16}$$

where

D_i^t = deficit in time period length *t* to user *i* [ft^3];

$n_{D_i^t>0}$ = the total number of deficits for user *i* over the simulation period

An evaluation of GWM results using the performance criteria of resilience and reliability provide valuable insight on the available groundwater considering current management. To accommodate future uncertainty in groundwater demand, the model runs may address various drought level conditions to achieve ranges for performance criteria

and management scenarios. Information obtained through this project serves to support stakeholder and management discourse regarding groundwater availability of the BSEA.

Chapter 4: Stochastic Pipe Break Results and Analysis

This chapter presents the results for the pipe break analysis, MODFLOW96 stochastic test scenarios and associated water budgets, as well as the MODFLOW-GWM test results and performance criteria analysis. Using the Wang et al. (2009) models and water distribution characteristic data provided by the City of Austin, PVC pipes had the highest break rates of the three pipe types represented. The integration of estimated pipe breaks and average flow losses from pipe main breaks (City of Austin, 2016) with Passarello's Altered Natural + Artificial recharge scenario (2011) yielded a maximum difference in Barton Springs discharge of -2.09 cfs (-0.06 cms). This maximum difference results from the minimum recharge scenario.

4.1 Pipe Break Analysis

An analysis of pipe data provided by the City of Austin was performed to obtain pipe characteristics (age, diameter, length) for cast iron, ductile iron, and PVC water distribution pipes within the boundaries of the BS GAM. Ultimately, the information required to update recharge rates is needed in cubic feet of water leaked per foot of pipe per month. The following results illustrate the process of obtaining leakage rates to update recharge files.

4.1.1 City of Austin Pipe Data

GIS data from the City of Austin was exported to Excel for statistical calculations. To code break rates by pipe type in Excel, each model (GAM) cell was labeled as the pipe type having the greatest length within cell boundaries. Out of 7,038 active cells in the BS GAM, the majority (4,941) have no water distribution pipes and therefore provide no artificial recharge from pressurized water mains to the Barton Springs segment of the Edwards Aquifer (Figure 15). Of the remaining 2,097 cells that house the City's water distribution system, the majority are PVC (739), followed by cast iron (576), ductile iron (402), and a variety of other pipe types comprise the remaining 380 cells (e.g. asbestos cement, galvanized iron, concrete, etc.). For reference, Appendix A contains a list of

additional pipe types present within the City of Austin's water distribution system. From 1999-2009, the water distribution system with the BS GAM grew from 1126 km (700 mi) to 1488 km (925 mi).

Additionally, the City of Austin (personal communication, 2016) provided quality assured, quality controlled (QA/QC) break data for 2010-2015. Losses per break range from 10 gallons (0.038 m^3) to 12,610,000 gallons (47,734 m^3) and averaged 20,529 gallons (77.7 m^3) per loss over the entire data set. Break occurrences per kilometer per year ranged from 0.21 (2012) to 0.26 (2011) and averaged 0.23 for the data set.

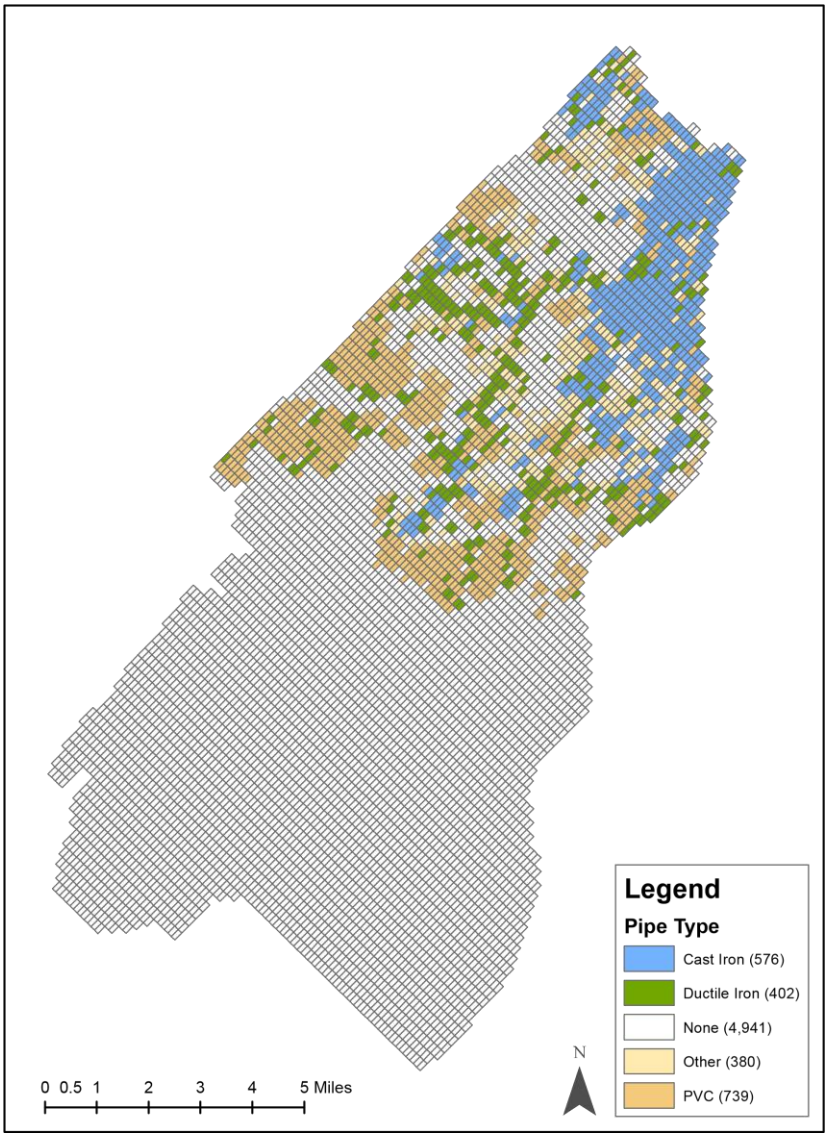

Figure 15. Pipe types by GAM cell (HydroID).

4.1.3 Wang et al. (2009) Model Results and Bayesian Updating

The regression models from Wang et al. (2009) applied to pipe material characteristics (age, diameter, length) from the City of Austin's GIS data set resulted in similar break rate ranges to the data presented by Wang et al. (2009). For cast iron, the break rates ranged from 0.11 to 33.50 breaks/km/year; for ductile iron, 0.31 to 29.30; for PVC, 0.08 to 14.60. The high annual break rates, with reference to the City of Austin's QA/QC rate, is a function of the pipe lengths, as a majority of Austin's pipes are less than 50 meters. As mentioned previously, Wang et al. (2009) observed higher break rates in pipes less than 50 meters compared to longer lengths for all pipe materials (Figure 10). In addition, due to the wide spread of pipe material input criteria, as a whole the data distributions were neither normal nor lognormal; thus, it was determined a full statistical analysis was beyond the project's scope and normality was assumed for the Monte Carlo analysis. Using a Monte Carlo analysis with 10,000 runs, results for minimum, mean, and maximum break rates for each pipe type were found, which differ from the original model application results due to the normality assumption (Table 3).

The Bayesian analysis was used to improve certainty, or "update," mean break rate probabilities using the QA/QC break rate of 0.23 (per km/year). "Prior" probabilities, before using the 0.23 break rate as the informative value, were 15% CI, 54% DI, and 31% PVC and are based on the ratio of pipe type over the total amount (Figure 16). It is worth noting the percentages used for the Bayesian analysis do not reflect the primary pipe material by BS GAM cell mentioned in the previous section. Updated probabilities, or "post probabilities" using Bayesian updating were 59% CI, 39% DI, and 2% PVC (Figure 17).

Table 3. Break rate results using Wang et al. (2009) models and Monte Carlo.

Break rate (per km/year)	**Cast Iron (CI)**	**Ductile Iron (DI)**	**PVC**
Minimum	0	0	0
Mean	2.23	3.56	6.69
Maximum	9.20	12.48	24.88

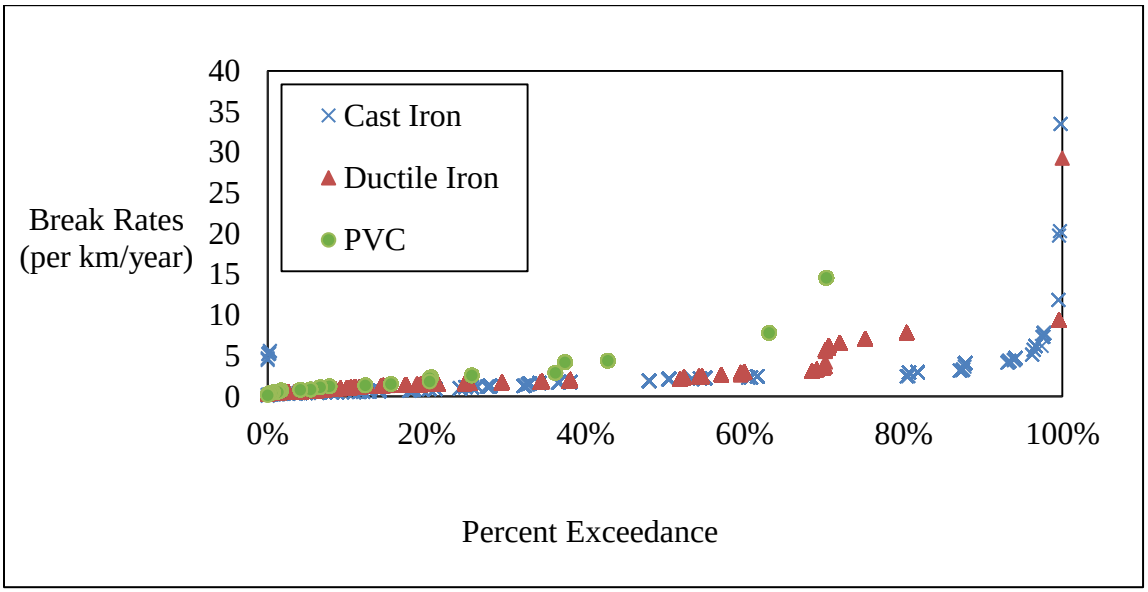

Figure 16. Break rates vs. probability exceedance for City of Austin water distribution data using Wang et al. (2009) models.

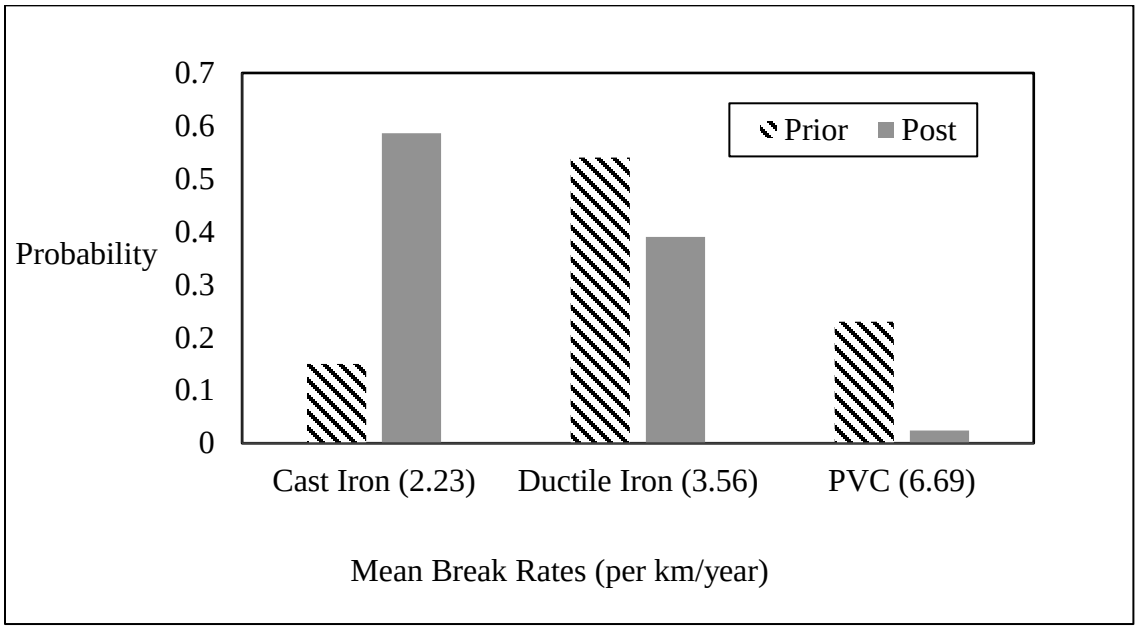

Figure 17. Break rates using Wang et al. (2009) models and Bayesian analysis.

4.1.4 Leakage Rates using Wang et al. (2009) models and Bayesian Analysis

Leakage rates required for the pipe break contribution are in cubic feet per foot of pipe length per month. Of 10,440 QA/QC water distribution break records from the City of Austin (2016) from 2009-2015, break losses range from 10 gallons to 12,610,000 gallons and average 20,524 gallons per break record. With an average loss of ~20,500 gallons, or 2,744 cubic feet per break, leakage rates range from 0.0 ft^3/ft/month to 1.73 ft^3/ft/month (Table 4). In comparison, leakage rates determined for Passarello's Altered Natural + Artificial Recharge scenario range from 1.42 ft^3/ft/month (February, 2005) to 3.60 ft^3/ft/month (August, 2001) for 1999-2008 and average 2.16 ft^3/ft/month. (2011).

Table 4. Leakage rates corresponding to unique break rates.

	Break Rate (per km/year)	**Leakage Rate (ft^3/ft/month)**
Minimum	0	0
QA/QC	0.23	0.02
Mean, CI	2.23	0.16
Mean, DI	3.56	0.25
Mean, PVC	6.69	0.47
Max, CI	9.2	0.64
Max, DI	12.48	0.87
Max, PVC	24.88	1.73
Mean, Altered N+A	---	2.16

4.2 Recharge Contribution by Scenario

To gauge model discharge outputs as a preliminary step for various recharge scenarios, recharge contributions by source were performed for each interpretation. The following sections describe the interpretations and their total contribution from artificial and natural sources. As mentioned previously, all natural sources, precipitation and streamflow, remain constant, while irrigation return flow and wastewater are constant artificial sources in each scenario. For the entire set of testing scenarios, the leakage contribution from wastewater and water mains ranged from 1.1 to 2%, compared to

Passarello's 3.8% for the Altered Natural + Artificial scenario (2011; Table 5). In addition, for the month with minimal recharge in each scenario, artificial recharge (irrigation return flow and leakage) ranged from 24.1% to 39.5%, compared to 54% for the Altered Natural + Artificial scenario (Table 6, Figure 18). For each scenario other than the Altered Natural + Artificial scenario, the month with minimal recharge was August, 2006. This difference is due to a constant monthly recharge rate in the new scenarios, as opposed to the variable rate in Passarello's scenario (2011).

4.2.1 Minimum Scenario

For the scenario with minimum recharge, a water leakage rate of zero was applied to the water distribution system to gain the minimum bound of uncertainty for the stochastic bounds. Artificial recharge, irrigation return flow (IRF) and wastewater leakage, contributed 2.4% of total recharge for the entire test and 24% of total recharge for August 2006, the month with minimal overall recharge.

4.2.2 QA/QC Data Scenario

As seen in Table 4, the QA/QC mean break rate of 0.23 breaks/km/year corresponds to a monthly leakage rate of 0.02 cubic feet per foot of pipe length, approximately two orders of magnitude lower than the average leakage rate for the Altered Natural + Artificial scenario. The QA/QC leakage rate corresponded to 0.03% of the total recharge contribution (1999-2008) and 25% of recharge for August 2006.

4.2.3 Mean and Maximum Scenarios with Bayesian Updating

Mean and maximum leakage rates by pipe type were assigned to HydroIDs according to their probability of occurring found through the Bayesian analysis. For comparison, maximum leakage were assigned to the same HydroID as their respective mean leakage rate. Of 2,097 active BS GAM cells with pipe lengths, CI rates were applied to 1,237 cells (39%), DI rates to 818 cells (39%), and PVC rates to 42 cells (2%). When appropriate, applied rates matched their original associated pipe material. Water leakage accounted for 0.11% and 0.60% of the total recharge for the mean and maximum recharge

scenarios, respectively. In addition, artificial sources represented 26% (mean) and 32% (maximum) of total recharge for August 2006.

4.2.4 Maximum Scenario

As artificial sources represented only 32% of total recharge for the maximum recharge scenario using the probability percentages applied in Bayesian updating, the application of maximum recharge rates was applied without probabilities from the Bayesian analysis. For this scenario, leakage rates by pipe material matched the primary pipe material of each BS GAM cell. As an assumption, cells with "OTHER" as their primary material were assigned the CI rate, the lowest of the three materials analyzed. Recharge from water leakage increased to 0.88% for total recharge in this scenario and the contribution from artificial sources increased to 40% for August 2006.

Table 5. Recharge contributions for individual testing scenarios.

Contribution Budgets, 1999-2008 (%)						
Source	**Altered N+A**	**Minimum**	**QA/QC**	**Mean (Bayes)**	**Maximum (Bayes)**	**Maximum (Not Bayes)**
IRF	1.3	1.3	1.3	1.3	1.3	1.3
Water Leakage	2.7	0	0.03	0.11	0.6	0.88
Wastewater Leakage	1.1	1.1	1.1	1.1	1.1	1.1
Streams	80	82	82	82	82	82
Precipitation	15	15	15	15	15	15

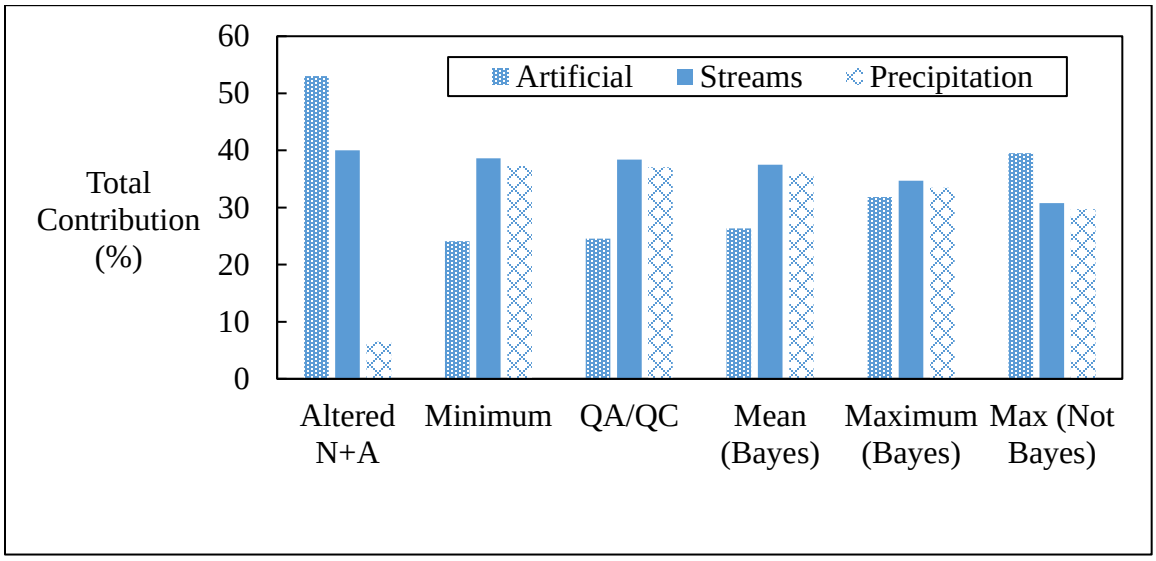

Figure 18. Recharge contribution by source for the month of minimal total recharge in each scenario.

Table 6. Recharge contribution by source for the month of minimal total recharge in each scenario.

Source	Altered N+A	Min	QA/QC	Mean (Bayes)	Max (Bayes)	Max (Not Bayes)
Minimum Recharge Month	Nov-99	Aug-06	Aug-06	Aug-06	Aug-06	Aug-06
Artificial	53	24	25	26	32	40
Streams	40	39	38	37	35	31
Precipitation	7	37	37	36	33	30

4.3 Model Results

After determining recharge contributions for each model scenario, the minimum and maximum (without Bayesian updating) scenarios were chosen to run with MODFLOW96 to determine bounds of uncertainty for a stochastic model. As expected from the water distribution leakage contribution analysis, both scenarios modeled discharge consistently lower than the Altered Natural + Artificial Scenario (Figure 19). To help convey differences between model scenario outputs, Figure 19 displays discharge in cubic feet per second. Modeled mean discharge for the minimum and maximum scenarios was 59.17 cfs (1.68 cms) and 59.52 cfs (1.69 cms), respectively. Comparatively, mean

modeled discharge for the Altered Natural + Artificial Recharge scenario was 60.80 cfs (1.72 cms). While the mean difference between the minimum and Altered Natural + Artificial scenarios was -1.63 cfs (-0.04 cms), the maximum difference was -2.09 cfs (-0.06 cms) for the month of October, 2007. Similarly, the mean difference for the maximum and Altered Natural + Artificial Recharge scenarios was -1.28 cfs (-0.03 cms) and the maximum difference was -1.50 cfs (-0.04 cms) in August, 2001.

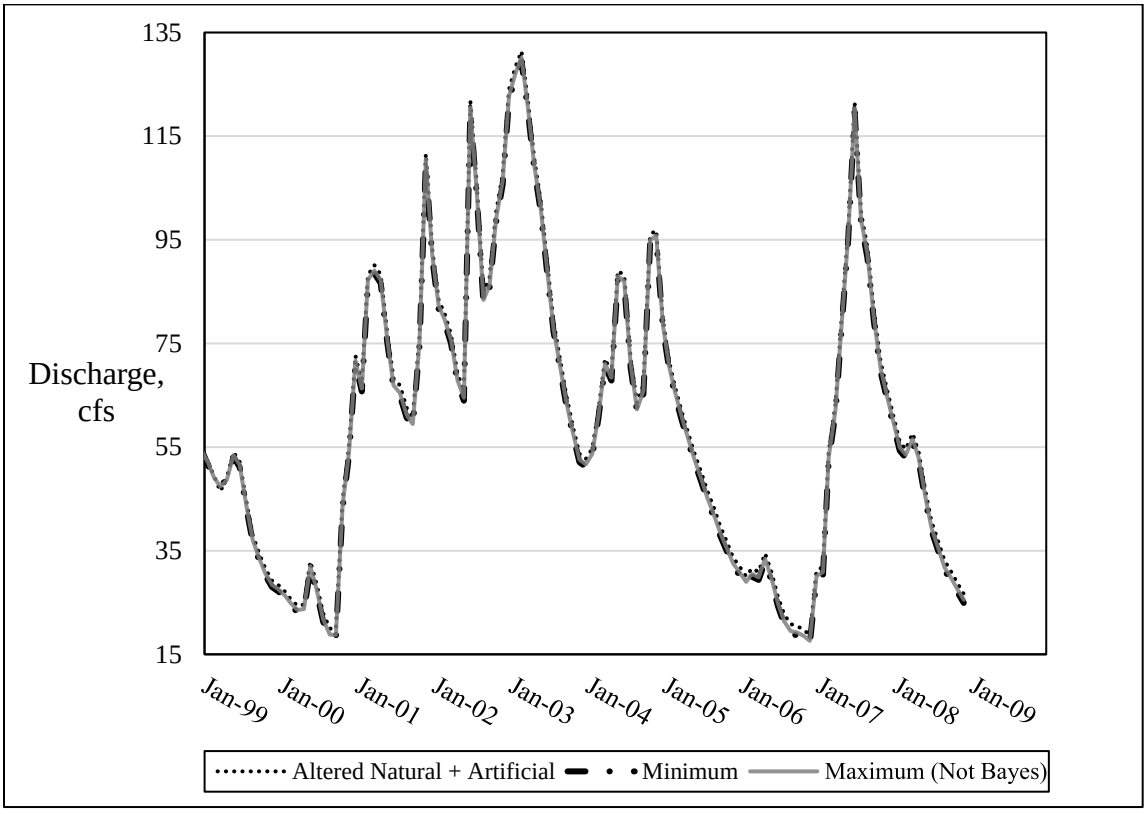

Figure 19. MODFLOW results for the Altered Natural + Artificial (Passarello, 2011), Minimum, and Maximum recharge scenarios.

4.4 Stochastic Pipe Break Analysis

The objective of the stochastic recharge analysis for this project was to provide bounds of uncertainty for the Altered Natural + Artificial recharge scenario (Passarello, 2011). While this purpose was achieved, results from this project indicate a pipe break analysis alone does not provide the full representation of artificial recharge to the Barton

Springs segment of the Edwards Aquifer. Even at maximum pipe break predictions (without Bayesian updating), water loss from water distribution pipes remained at almost half (2% compared with 3.8%) of that determined from Passarello's flow loss methods (2011). These results indicate there is a significant amount of water loss within the Barton Springs Edwards Aquifer system not captured in this project's pipe break analysis. As the pipe break analysis, as well as work orders provided by the City of Austin, only capture major breakages, small cracks and corrosion most likely contribute a majority of water lost from the water distribution system.

The comparison of recharge contributions from various modeling scenarios, including Passarello's Altered Natural + Artificial interpretation, provided the best indication of MODFLOW-96 discharge results for Barton Springs. Once minimum and maximum (no Bayesian updating) model runs were performed and compared with Passarello's Altered Natural + Artificial recharge interpretation, a comparison of total recharge from each additional scenario indicated the anticipated model results would not produce a greater difference in discharge than -2.09 cfs (-0.06 cms).

Chapter 5: GWM Results and Analysis

The purpose of this section is to discuss the results and analysis for optimized withdrawals in the BSEA using multiple MODFLOW-GWM simulations. This section includes a sensitivity analysis performed on head closure criterion of the SIP solution file and modeling scenarios using both the linear and sequential linear programming solution attempts as well as the MODFLOW-GWM results and analysis. MODFLOW-GWM was applied to the Altered Natural + Artificial and Natural + Artificial recharge scenarios for this project using both 90 well objectives running over the entire simulation and 450 well objectives (90 wells with biennial objectives). For the Altered Natural + Artificial scenario with 90 well objectives, GWM was not able to yield a solution for the Alarm Drought head constraint, but resulted in 16.9 – 87.5 % withdrawals for the Critical Drought - Emergency Response head constraints (Table 9). The more discretized model with 450 objectives resulted in 66.8% of the total objective withdrawn (Table 10). For the Natural + Artificial interpretation, GWM tests resulted in 65.0 - 100 % of desired withdrawals for the 90 well objective tests using all DTM head constraints and 94.4% of the total 450 objectives with the Alarm Drought constraint (Table 9). Reliability and resilience were assessed for the 450 well objective model runs in each scenario. The Altered Natural + Artificial scenario with the Critical Drought constraint resulted in 40% reliability and 66.7 resilience while the Natural + Artificial scenario with the Alarm Drought constraint achieved 80% reliability and 100% resilience (Table 10).

5.1 Well Objectives

Total pumping from 1999-2008 increased 144% from Passarello's updated well file to the GWM simulation (Table 7; 2011). The greatest annual pumping occurred in 2005 with approximately 2.08 billion gallons withdrawn; 22% less than annual withdrawals for the GWM simulation. Passarello repeated the 2005 withdrawals from 2006-2008 for all simulations due to available data (2011).

Table 7. Annual withdrawals, Passarello (2011) and GWM.

Year	Gallons Pumped, Passarello (2011)	Well Discharge, cfs (Passarello, 2011)	Gallons Pumped, GWM	Well Discharge, cfs (GWM)
1999	1,562,683,907	6.6	2,688,247,597	11.4
2000	1,673,448,686	7.1	2,688,247,597	11.4
2001	1,766,597,509	7.5	2,688,247,597	11.4
2002	1,806,107,505	7.7	2,688,247,597	11.4
2003	1,777,972,112	7.5	2,688,247,597	11.4
2004	1,666,543,726	7.1	2,688,247,597	11.4
2005	2,084,538,845	8.8	2,688,247,597	11.4
2006	2,084,538,845	8.8	2,688,247,597	11.4
2007	2,084,538,845	8.8	2,688,247,597	11.4
2008	2,084,538,845	8.8	2,688,247,597	11.4
Total	18,591,508,822	-	26,882,475,972	-

5.2 Sensitivity Analysis

The original BS GAM model (Scanlon et al., 2001) and resulting interpretations for this project uses a head closure criterion (HCLOSE) value of 0.1 in the strongly implicit procedure (SIP) solution file. The HCLOSE criterion sets a value for convergence at which head change iterations stop once the value is met. As suggested by Paul Barlow of the USGS (personal communication, 2016), a smaller HCLOSE criterion improves model accuracy. As a result of this discussion, a sensitivity analysis was performed on a demonstration model to provide a range of percent withdrawal objectives met for the tests using the linear programming (LP) solution file for GWM. In addition, sequential linear programming (SLP) was performed on one of the demonstration tests to observe discrepancies in GWM objective outcomes. The demonstration GWM test used for the sensitivity analysis included Passarello's Natural + Artificial recharge scenario (2011).

For the LP demonstration file, all 90 wells were specified to pump over the entire model run according to the Alarm Drought head constraint of 478.4 feet, thus producing

90 final outputs in the model's global file. SIP values tested ranged from 0.001 to 0.1 with a total percent of objective met ranging from 60.7% to 64.9%, respectively, indicating an increased HCLOSE value resulted in an increased percent of objective met (Table 8). In addition, the SLP and LP model runs using HCLOSE values produced comparable results (Table 8). In addition, subsequent GWM scenarios for this project use the HCLOSE value of 0.1, the original value specified for the BS GAM (Scanlon et al., 2001).

Table 8. GWM sensitivity analysis results.

Run Name	Head Closure Criterion (HCLOSE)	Percent of Objective Met
LP1	0.001	60.7
LP2	0.01	61.4
LP3	0.1	64.9
SLP1	0.001	60.7

5.3 GWM Scenarios and Results

Initial attempts to run the Altered Natural + Natural scenario in GWM with 90 well objectives and the Alarm Drought constraint yielded "no feasible solution". As a result, the Altered Natural + Artificial and Natural + Artificial recharge scenario (Passarello, 2011) were run with all drought constraints to gauge the various effects of recharge quantities on pumping. As mentioned in previous sections, the Natural + Artificial recharge scenario has approximately 160% higher recharge than the Altered Natural + Artificial scenario due to the use of higher infiltration rates (Table 10). Passarello's Natural + Artificial scenario (2011) met 100% of the withdrawal objectives at the Critical Drought head constraint while the Altered Natural + Artificial scenario (2011) met only 87.52% of the total objective by the Emergency Response constraint (Table 9).

To provide a more discretized output for the GWM Global file than the initial 90 well objective scenarios, a new well file was created that included all 90 wells with biennially withdrawal optimization for the total model time of 10 years, resulting in a total of 450 wells. This well discretization allows for output processing of each well on a

biennial basis as opposed to the end of the 10-year model run for the simulations using the 90 well objectives. Initially, 900 well objectives were attempted to achieve annual discretization, but the processing space required exceeded the author's 2 terabyte (TB) capacity. LP model runs averaged a 48 hour run time and 1.5 TB of space per model, while an attempted SLP run exceeded 2 TB. Due to the similar results of the SLP and LP demonstration scenarios and data constraints, subsequent tests were run using the LP solution. The following sections describe the results achieved for the 450 well constraints using both the Altered Natural + Artificial and Natural + Artificial scenarios (Table 10).

Table 9. GWM results, 90 wells for all DTM head constraints.

HCLOSE = 0.1	**Lovelady Monitoring Well Level**	**Altered N+A**	**N+A**
		Percentage Withdrawn (90 wells)	
Alarm Drought – Stage II	478.4 feet	No solution	65
Critical Drought – Stage III	462.7 feet	16.9	100
Exceptional Drought - Stage IV	457.1 feet	60.7	100
Emergency Response	453.4 feet	87.5	100

Table 10. GWM results, 450 wells (90 bienniel wells) for various DTM head constraints.

Scenario	**Total Recharge (10^9 ft^3)**	**Percent Objective Met**	**Reliability (%)**	**Resilience (%)**
Altered N + A (Alarm Drought)	22.1	No solution found	N/A	N/A
Altered N+A (Critical Drought)	22.1	66.8	40	66.7
N + A (Alarm Drought)	35.5	94.4	80	100

5.3.1 Altered Natural + Artificial Scenario

The Altered Natural + Artificial scenario was not able to meet the pumping objectives with the Alarm Drought constraint at the Lovelady Monitoring Well. Specifically, the head constraint was not met from November 1999 – October 2000, April 2006, June 2006 – November 2006, and December 2008 (Figure 20). It should be noted these exact months were not met when this scenario was attempted with 90 well objectives. Optimal withdrawal rates were achieved for the Critical Drought constraint, which corresponds to 20 cfs at Barton Springs for the BSEACD's DTM, resulting in the 11.4 cfs objective being reduced to approximately 1.9 cfs for 1999 and 2000, 11.2 cfs for 2003 and 2004, and 2.1 cfs for 2005 and 2006 (Figure 21). While only 17.1 and 18.2% of the biennial objective was met for 1999/2000 and 2005/2006, respectively, 66.8% of the overall objective was achieved for the Critical Drought constraint (Table 10; Figure 24).

For 1999 and 2000, minimal discharge at Barton Springs for Passarello's simulation (2011) fell below the 20 cfs Critical Drought level to 19.3 cfs in October 2000, while the optimized simulation kept discharge at 24.6 cfs for the same month (Figure 21). Similarly, the Barton Springs fell to its lowest overall discharge in December 2006 for both simulations; while the original simulation (Passarello, 2011) dropped to 18.3 cfs, the optimized simulation kept discharge above the Critical Drought level and achieved 24.6 cfs (Figure 21). Overall, the Altered Natural + Artificial simulation resulted in 40% reliability and 66.67% resilience (Table 10).

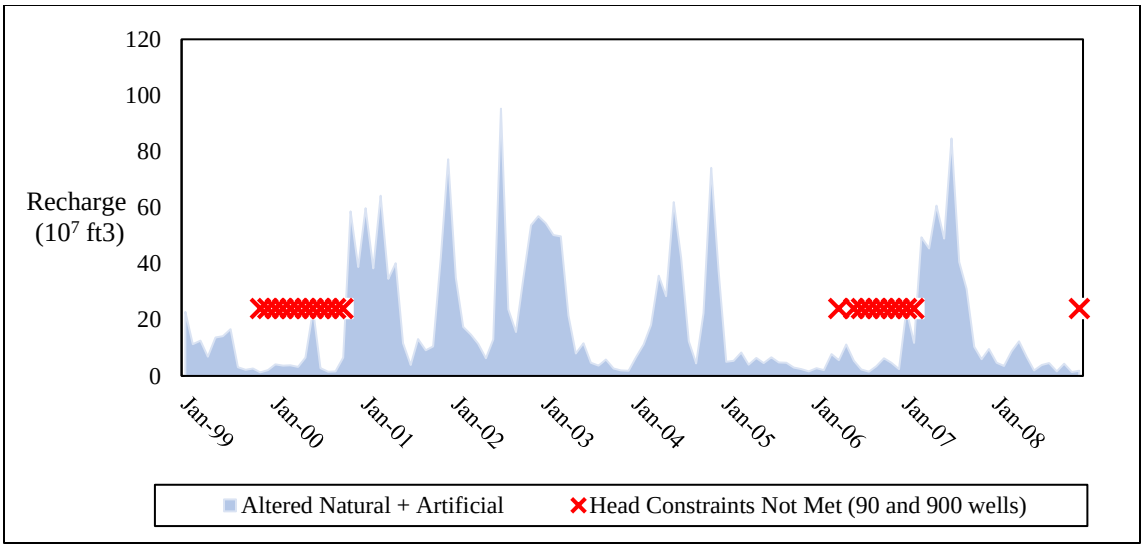

Figure 20. Monthly recharge and unmet constraints for the Altered Natural + Artificial scenario.

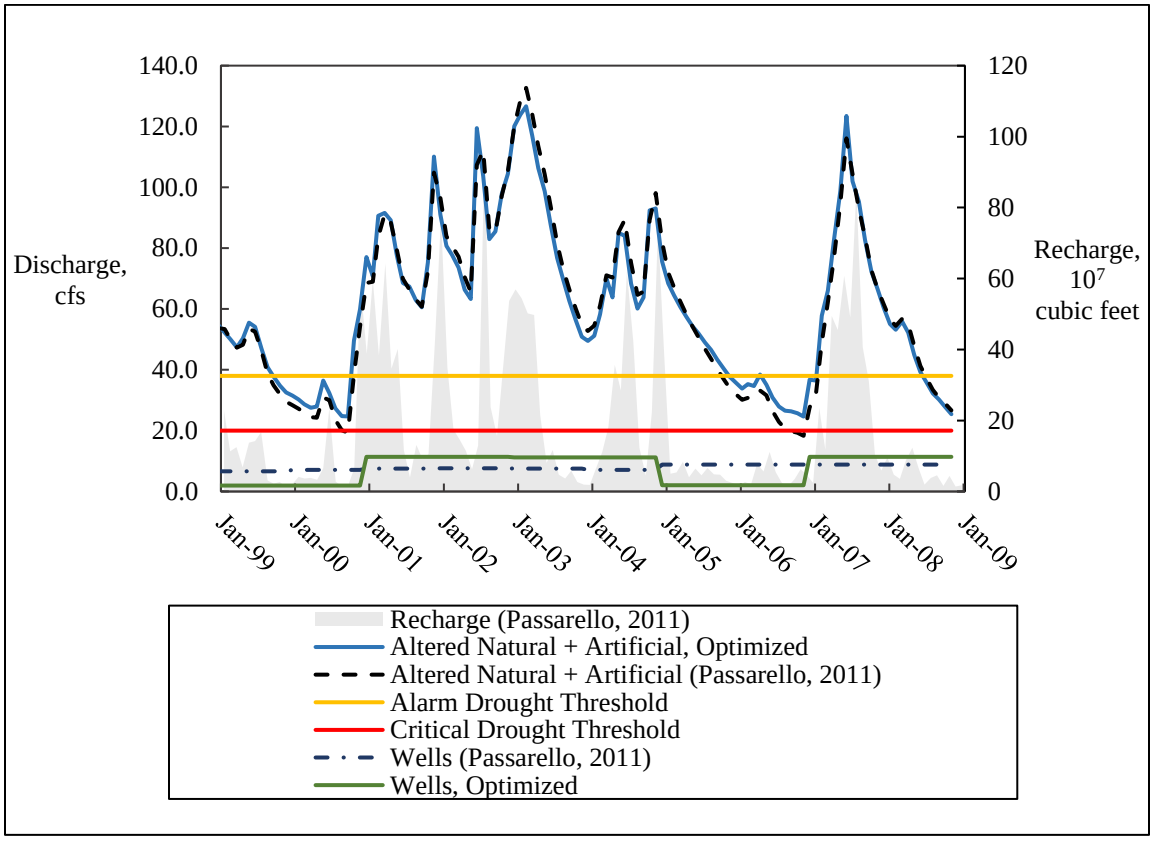

Figure 21. Recharge, well withdrawals, and springflow discharge for optimized vs. non-optimized Altered Natural + Artificial simulations.

5.3.2 Natural + Artificial Scenario

For the Alarm Drought head constraint on the Lovelady Monitoring Well, the Natural + Artificial scenario met 94.4% of the withdrawal objectives, with 1999 and 2000 as the only reduction (Table 10). For 1999 and 2000, the optimal pumping rate was 64.9% of the objective, resulting in a withdrawal rate of 7.4 cfs (Figure 24; Figure 22). In the non-optimized simulation (Passarello, 2011), discharge at Barton Springs fell to its minimum springflow of 38.5 cfs in April 2000, thus staying above the 38 cfs Alarm Drought trigger throughout the simulation. The optimized simulation, while pumping at a lower rate, produced a 38.2 cfs springflow for April 2000 (Figure 22). Reliability and resilience were 80% and 100%, respectively, for the Natural + Artificial GWM simulation (Table 10).

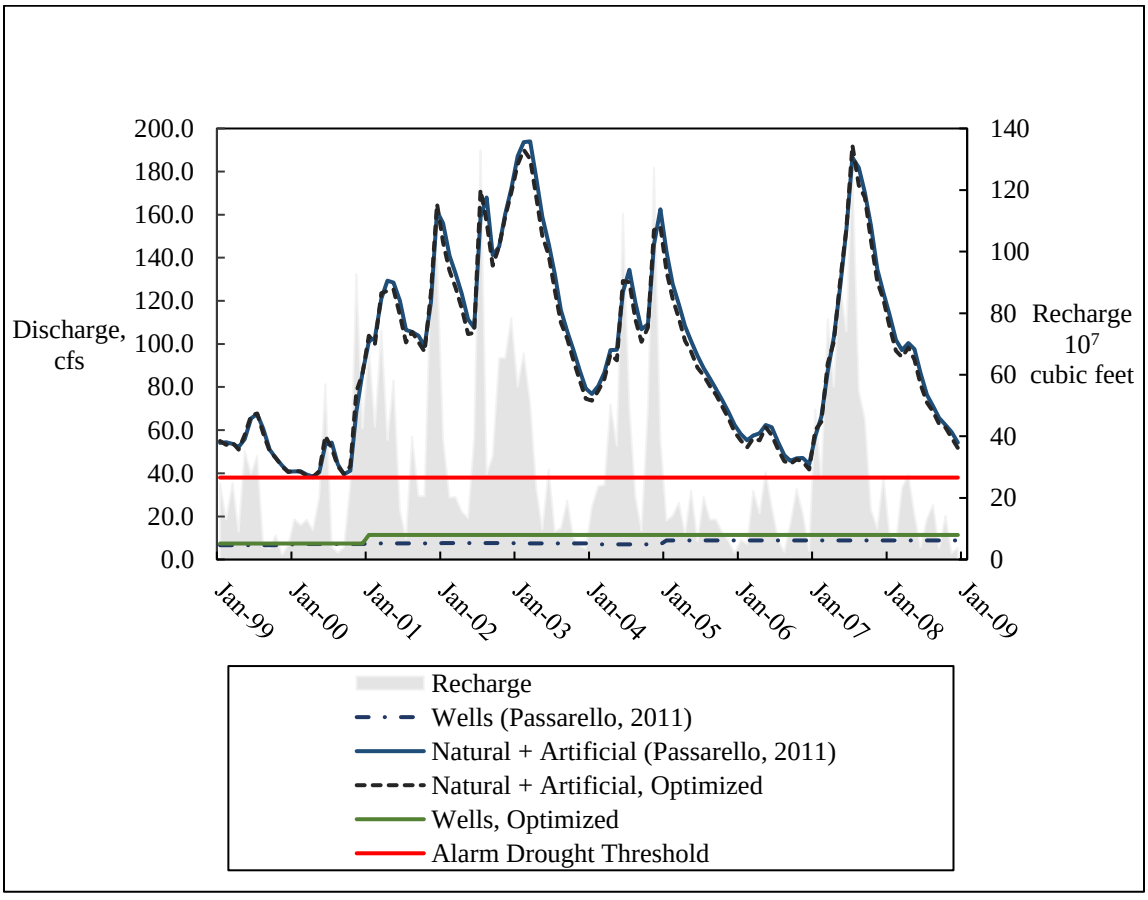

Figure 22. Recharge, well withdrawals, and springflow discharge for optimized vs. non-optimized Natural + Artificial simulations.

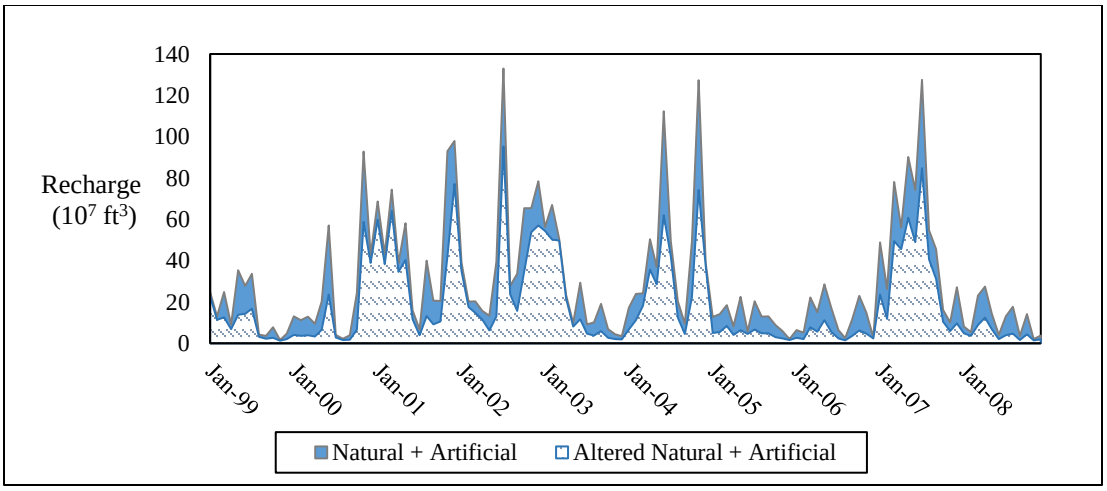

Figure 23. Monthly recharge inputs for Altered N + A and N + A scenarios (Passarello, 2011).

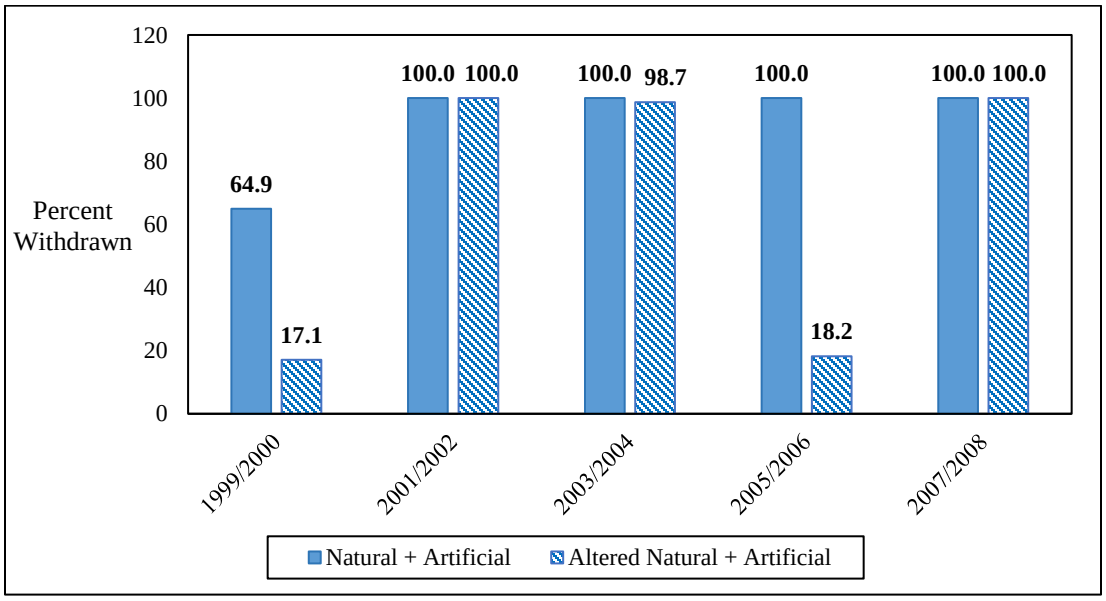

Figure 24. Percent of biennial objective withdrawn by GWM scenario.

5.4 GWM Analysis

The objective of combining MODFLOW-GWM with the BS GAM simulations was to provide a management application to various recharge interpretations of the BSEA groundwater flow model. The GWM simulations of this project, though limited by data space, indicate the sensitivity of annual withdrawals within GWM to recharge at all stress periods within the model. Lovelady Monitoring Well constraints, in particular the Critical Drought Constraint in the Altered Natural + Artificial 450 well objective simulation, kept Barton Springs discharge levels above the corresponding springflow drought trigger and proved sufficient for future work with the GWM package developed for this research.

The lower discharge levels at Barton Springs for the minimum springflow in the Natural + Artificial simulation may be due to different methods used to calculate flow at both Barton and Cold Springs by the author and Passarello (2011). For this research, the author employed Scanlon et al.'s (2001) method, with Cold Springs representing 6% of the total discharge from the drains in each time step. Passarello's calculations were performed through a computed algorithm that a fluctuating value for Cold Springs.

As successful GWM model runs resulted in relatively long run times and space requirements, it is best to discuss groundwater management with respect to this project's model with a broad perspective. Although well objectives were met at full capacity for some of the time periods, the coarse discretization of biennial, rather than monthly well withdrawals, inadequately recognizes peak demands on the aquifer, particularly during drought periods. Future work, with a particular focus on initial model recharge, as well as monthly discretized wells, may provide more sufficient outputs with respect to performance criteria. In addition, while better discretized objectives allow for more adequate management integration, the longer run times required for these models are not conducive to iterative round-table interaction with model inputs and outputs. Nevertheless, the results from this project, particularly with respect to the annual withdrawal objective and performance criteria assessment, will aid management and stakeholder dialogue and can help to shape future research regarding the BSEA.

Chapter 6: Conclusions

The research presented in this thesis describes the methodology, results, and analysis for developing a stochastic pipe break analysis for urban recharge in the BS GAM and applying the pipe break analysis to previous model scenarios and MODFLOW-GWM. This thesis achieved the objectives defined in the Introduction as follows:

1. A stochastic method for pipe break analysis in the BS GAM was developed and analyzed.
2. Multiple MODFLOW Groundwater Management (GWM) packages were constructed and analyzed with various recharge scenarios.
3. Withdrawal objectives for the BSEA were maximized according to drought trigger constraints set by the BSEACD in the developed GWM packages.
4. GWM results were evaluated using the performance criteria reliability and resilience.

Multiple modeling objectives and scenarios may be applied to the BS GAM to measure urban recharge contributions integrate groundwater management decisions simultaneously. Results of the pipe break analysis indicate major pipe breaks, such as those involving necessary excavation and repair, to not be the significant source of leakage from water distribution mains. Rather, a majority of artificial recharge is likely a result of undetected leakage, such as minor breaks, corrosion, or cracks. MODFLOW-GWM, which was used to optimize maximum groundwater withdrawals according to Drought Trigger Methodology constraints set by the BSEACD, provided insight to the use of groundwater models for groundwater management decisions. As a GWM model has not been developed for the BSEACD until this project, the model developed and discussed in this thesis serves as a baseline from which various pumpage, head constraints, and recharge scenarios may be altered to evaluate optimization and model sensitivity. The results from this project will serve to aid management and stakeholder discussions, should the BSEACD pursue further development of GWM modelling scenarios.

6.1 Limitations

The research presented in this thesis included the development of stochastic modeling and MODFLOW-GWM packages for the original BS GAM (Scanlon et al., 2001) modified for artificial recharge (Passarello, 2011). The limitations of the packages created through this research are presented as follows:

1. The Wang et al. (2009) regression models were developed using a specific data set. The adapted models in this research do not address any change in environmental conditions to the present study area, such as climate or soil types.
2. The resolution of well withdrawal optimization for the GWM model package is discretized on a biennial basis due to computational capacity.

6.2 Future Work

This project allowed for the insight of pipe break analysis on urban recharge and the application of groundwater management simulations through MODFLOW-GWM. Numerous opportunities exist, from statistics to modeling, in the realm of pipe break analysis for the City of Austin's water distribution system. For example, an extensive study could be performed, in partnership with the City of Austin, to gather pipe characteristics in partnership with break work orders and use this information to develop regression models unique to Austin. In addition, stochastic methodology may be applied to the BS GAM at TACC, which would allow for increased modeling capabilities.

The brief application of GWM in this project provided insight to multiple future applications of the program in conjunction with the BS GAM. As mentioned previously, future work GWM and the BS GAM may involve a sensitivity analysis in regard to recharge during the model's initial time steps, as well as a finer time discretization on pumping wells. In addition, pumpage, constraints, and even economics may be altered and researched to further develop GWM for the BS GAM. With greater space capacity, SLP programming should be assessed as a comparison to the LP simulations run for this project. Advanced computing systems, in addition to GWM package refinement, will only serve to

aid communication and decisions among stakeholder interest groups and governing agencies.

References

Ahfeld, D. P., Barlow, P. M., & Mulligan, A. E. (2005). *GWM-A Ground-Water Management Process for the U.S. Geological Survey Modular Ground-Water Model (MODFLOW-2000)* (Open-File Report No. 2005-1072) (p. 124). U.S. Geological Survey.

American Society of Civil Engineers. (2013). 2013 Report Card for America's Infrastructure: Drinking Water. Retrieved in 2016 from www.infrastructurereportcard.org.

American Water Works Association. (2016). *Buried no longer: confronting America's water infrastructure challenge.* (p. 37).

Alvisi, S., & Franchini, M. (2010). Comparative analysis of two probabilistic pipe breakage models applied to a real water distribution system. *Civil Engineering and Environmental Systems*, 27(1), 1-22.

Andreou, S. A., & Marks, D. H. (1986). Maintenance planning strategies for large diameter cast-iron mains. (pp. 365-372). Presented at the AWWA Conference Synopsis.

Austintexas.gov. (2016). Watershed Protection Department. Retrieved from www.austintexas.gov/department/salamanders.

Barlow, P. (2016). Personal communication. U.S. Geological Survey.

Barrett, M. E., & Charbeneau, R. J. (1996). *A Parsimonious Model for Simulation of Flow and Transport in a Karst Aquifer* (Technical Report No. 269). Center for Research in Water Resources.

Bayes, Mr., & Price, Mr. (1763). An Essay towards Solving a Problem in the Doctrine of Chances. By the Late Rev. Mr. Bayes, F.R.S. Communicated by Mr. Price, in a Letter to John Canton, A.M.F.R.S. *Phil. Trans., 53*, 370-418.

BSEACD. (2016). Barton Springs / Edwards Aquifer Conservation District. Retrieved from www.bseacd.org.

Caran, C., & Baker, V. (1986). Flooding along the Balcones Escarpment, Central Texas. In *The Balcones Escarpment, Geology, Hydrology, Ecology, and Social*

Development in Central Texas.

City of Austin, Texas. (2016). Personal communication.

City of Austin, Texas. (2016). Quality assured, quality controlled (QA/QC) pipe break work orders. Unpublished raw data.

Clark, R. M., Stafford, C. L., & Goodrich, J. A. (1982). Water distribution systems: A spatial and cost evaluation. *Journal of Water Resources Planning and Management Division, 108*(3), 243-256.

Cox, D. R. (1972). Regression models and life tables. *Journal of the Royal Statistical Society, 34*(B), 187-220.

Duffy, M. (2016). *Challenges in the Water Industry: Infrastructure and its Role in Water Supply* [White paper]. Retrieved from American Water.

EAA. (2016). Edwards Aquifer Authority. Retrieved from www.edwardsaquifer.org

Harbaugh, A. W., Banta, E. R., Hill, M. C., & McDonald, M. G. (2000). *MODFLOW-2000, The U.S. Geological Survey modular ground-water model - user guide to modularization concepts and the ground-water flow process* (Open-File Report No. 00-92) (p. 113). U.S. Geological Survey.

Harbaugh, A. W., & McDonald, M. G. (1996). *User's documentation for MODFLOW-96, an update to the U.S. Geological Survey modular finite-difference ground-water flow model* (Open-File Report No. 96-485). U.S. Geological Survey.

Hashimoto, T., Stedinger, J.R., & Loucks, D. P. (1982). Reliability, Resiliency and Vulnerability Criteria for Water Resource System Performance Evalution. *Water Resources Research. 18* (1), 14-20.

Hauwert, N. M., Johns, D. A., Sansom, J. W., & Aley, T. J. (2002a). Groundwater Tracing of the Barton Springs Edwards Aquifer, Travis and Hays Counties, Texas (Vol. 52, pp. 377-384). Gulf Coast Associations of Geological Societies Transactions.

Hovorka, S. D., Mace, R. E., & Collins, E. (1998). *Permeability Structure of the Edwards Aquifer, South Texas - Implications for Aquifer Management* (Report of Investigations No. 250) (p. 55). The University of Texas at Austin, Bureau of Economic Geology.

Hunt, B. B., Smith, B. A., Beery, J., Johns, D., & Hauwert, N. M. (2006). *Summary of 2005 Groundwater Dye Tracing, Barton Springs Segment of the Edwards Aquifer, Hays and Travis Counties, Central Texas* (Report of Investigations No. 2006-0530). Barton Springs / Edwards Aquifer Conservation District. Retrieved from www.bseacd.org.

Hunt, B. B., Smith, B. A., Slade, Jr., R. M., Gary, R. H., & Holland, W. F. (2012). Temporal Trends in Precipitation and Hydrologic Responses Affecting the Barton Springs Segment of the Edwards Aquifer, Central Texas. In *Gulf Coast Association of Geological Societies*. Austin, Texas.

Hutchinson, W.R., & Hill, M.E. (2011). *Report: Recalibration of the Edwards (Balcones Fault Zone) Aquifer – Barton Springs Segment – Groundwater Flow Model.*

Hutson, S.S., Barber, N. L., Kenny, J. F., Lindsey, K. S., Lumia, D. S., & Maupin, M. A. (2004). *Estimated Use of Water in the United States in 2000* (Circular 1268). U.S. Geological Survey.

Jacobs, P., & Karney, B. (1994). GIS development with application to cast iron water main breakage rate. *In 2nd international conference of water pipeline systems.* BHR Group Ltd, Ediburgh, Scotland.

Kettler, A. J., & Goulter, L. C. (1985). An analysis of pipe breakage in urban water distribution networks. *Canadian Journal of Civil Engineering*, *12*, 286–293.

Klemes, V., Srikanthan, R., & McMahon, T. A., (1981). Long-memory Flow Models in Reservoir Analysis: What is their Practical Value? *Water Resources Research, 17*(3), 737-751.

Konikow, L.F. (2013). *Groundwater depletion in the United States (1900-2008)* (Scientific Investigations Report No. 2013-5079) (p.63). U.S. Geological Survey.

Le Gat, Y., & Eisenbeis, P. (2000). Using maintenance records to forecast failures in water networks. *Urban Water, 2*, 173-181.

Leung, R. (2008). Downscaling for Assessing Climate Impacts: Examples and Future Directions. In *Climate Change Impacts on Texas Water*. Austin, Texas.

LGB-Guyton and Associates. (1994). *Edwards Aquifer Ground-Water Divides Assessment, San Antonio Region, Texas* (No. 95-01) (p. 35). Austin, Texas:

Edwards Underground Water District.

Lindgren, R. J. (2006). *Diffuse-flow conceptualization and simulation of the Edwards Aquifer, San Antonio Region, Texas* (Scientific Investigations Report No. 2006-5319). U.S. Geological Survey.

Lindgren, R. J., Dutton, A. R., Hovorka, S. D., Worthington, S. R. H., & Painter, S. L. (2004). *Conceptualization and simulation of the Edwards Aquifer, San Antonio Regions, Texas* (Scientific Investigations Report No. 2006-5277). U.S. Geological Survey.

Loaiciga, H. (2008). Climate Change, Growth, and Managing the Edwards Aquifer. In *Climate Change Impacts on Texas Water*. Austin, Texas.

Mace, R. (2008). Will Climate Change Affect the Aquifers of Texas? In *Climate Change Impacts on Texas Water*. Austin, Texas.

Mailhot, A., Pelletier, G., Noel, J.-F., & Villeneuve, J.-P. (2000). Modeling the evolution of the structural state of water pipe networks with brief recorded pipe break histories: Methodology and application. *Water Resources Research, 36*(10), 3053-3062.

Marks, D. Andreou, S. & Park, C. (1985). Predicting Urban Water Distribution Maintenance Strategies: A Case Study of New Haven, Connecticut. *EPA Draft Report.*

McDonald, M.G., & Harbaugh, A.W. (1984). *A modular three-dimensional finite-difference ground-water flow model.* (Open File Report number 83-875). U.S. Geological Survey.

McDonald, M.G., & Harbaugh, A.W. (1988). A modular three-dimensional finite-difference ground-water flow model. In *Techniques of Water-Resources Investigations of the United States Geological Survey* (Vol. Book 6, Chapter A1, p. 586). U.S. Geological Survey.

McMahon T.A., Adeloye, A.J., & Zhou, S. (2006). Understanding Performance Measures of Reservoirs. *Journal of Hydrology, 324* (2006), pp. 359-382.

McMullen, L. D. (1982). In *Advanced concepts in soil evaluation for exterior pipeline corrosion.* Miami, FL.

Nielsen-Gammon, J. W. (2008). What Does the Historic Climate Record in Texas Say about Future Climate Change? In *Climate Change Impacts on Texas Water*. Austin, Texas.

NOAA. (2016). Austin Climate Summary. Retrieved from http://www.srh.noaa.gov/images/ewx/climate/ausclisum.pdf

North, G. (2008). Presentation at Climate Change Impacts on Texas Water. Presented at the Texas State Capitol Extension, Austin, Texas.

Painter, S. L., Sun, A., & Green, R. T. (2007). *Enhanced characterization and representation of flow through karst aquifers - Phase II, Revision 1: San, Antonio, Southwest Research Institute, final technical report prepared for Southwest Florida Water Management District, Brooksville, FL., and Edwards Aquifer Authority under SWRI Project 20-11674*.

Passarello, M. C. (2011, May). *New Methods for Quantifying and Modeling Estimates of Anthropogenic and Natural Recharge: A Case Study for the Barton Springs Segment of the Edwards Aquifer, Austin, Texas* (Master of Science in Geological Sciences). University of Texas at Austin.

Scanlon, B. R., Mace, R. E., Barrett, M. E., & Smith, B. A. (2003). Can we simulate regional groundwater flow in a karst system using equivalent porous media models? Case Study, Barton Springs Edwards Aquifer, USA. *Journal of Hydrology, 276*, 137-158.

Scanlon, B. R., Mace, R. E., Smith, B., Hovorka, S., Dutton, A. R., & Reedy, R. C. (2001). *Groundwater Availability of the Barton Springs Segment of the Edwards Aquifer, Texas: Numerical Simulations through 2050*. The University of Texas at Austin, Bureau of Economic Geology: Lower Colorado River Authority, contract no. UTA99-0.

Senger, R. K., & Kreitler, C. W. (1984). *Hydrogeology of the Edwards Aquifer, Austin Area, Central Texas* (Report of Investigations No. 141) (p. 35). The University of Texas at Austin, Bureau of Economic Geology.

Shamir, U., & Howard, C. D. D. (1979). An analytic approach to scheduling pipe replacement. *Journal - American Water Works Association, 71*(5), 248-258.

Singh, V. (2008). Spatial-temporal Changes on Rainfall and Temperature and their Impact on Water Resources in Texas. In *Climate Change Impacts on Texas Water*. Austin, Texas.

Slade, Jr., R. M., Dorsey, M. E., & Stewart, S. L. (1986). *Hydrology and water quality of the Edwards Aquifer associated with Barton Springs in the Austin area, Texas* (Water-Resources Investigations Report No. 86-4036) (p. 124). U.S. Geological Survey.

Slade, Jr., R. M., Ruiz, L., & Slagle, D. (1985). *Simulation of the flow system of Barton Springs and associated Edwards Aquifer in the Austin area, Texas* (Water-Resources Investigations Report No. 85-4299) (p. 48). U.S. Geological Survey.

Smith, B. A., & Hunt, B. B. (2004). *Evaluation of the sustainable yield of the Barton Springs segment of the Edwards Aquifer, Hays and Travis Counties, Central Texas*. Barton Springs / Edwards Aquifer Conservation District.

Smith, B. A., Hunt, B. B., & Holland, W. F. (2013). *Drought Trigger Methodology for the Barton Springs Aquifer, Travis and Hays Counties, Texas* (Report of Investigations No. 2013-1201). Austin, Texas: Barton Springs / Edwards Aquifer Conservation District.

Teasley, R.L. (2009). *Evaluating Water Resource Management in Transboundary River Basins using Cooperative Game Theory: The Rio Grande/Bravo Basin.* The University of Texas at Austin, Austin, Texas.

Texas Water Development Board (TWDB). (2016). Rules and Statutes. Retrieved from http//.www.twdb.texas.gov/groundwater

U.S. Climate Data. (2016). Climate Austin-Texas. Retrieved from http://www.usclimatedata.com/climate/austin/texas/united-states/ustx2742

US EPA. (2016). Sole Source Aquifers for Drinking Water. Retrieved from http://www.epa.gov/dwssa

U.S. Geological Survey. (2015). Groundwater use in the United States. Retrieved from http://water.usgs.gov/edu/wugw.html.

Walski, T. M., & Pelliccia, A. (1982). Economic analysis of water main breaks. *Journal - American Water Works Association, 74*(3), 140-147.

Wang, Y., Zayed, T., & Moselhi, O. (2009). Prediction models for annual break rates of water mains. *Journal of Performance of Constructed Facilities*, *23*, 47-54.

Washington, W. (2008). The Development and Use of Climate Models for Understanding Future Trends of Water Availability in the West. In *Climate Change Impacts on Texas Water*. Austin, Texas.

Wiles, T.J., & Sharp, J.M., Jr. (2008). The secondary permeability of impervious cover. *Environmental and Engineering Geoscience*, *14*(4), 251-265.

Yamijala, S., Guikema, S. D., & Brumbelow, K. (2009). Statistical models for the analysis of water distribution system pipe break data. *Reliability Engineering and Systems Safety*, *94*(2), 282-293.

Zayed, T. & Halpin, D. (2005). Pipe Construction Productivity Assessment. *ASCE Journal of Construction Engineering and Management*, *131*(6), 705-714.

Appendix A

Table 11. Permitted and actual pumpage for the BSEACD, 1999-2006 (Hunt et al., 2006).

	1990	1991	1992	1993	1994	1995	1996	1997	1998
No. Permittees	52	62	74	75	77	91	86	95	96
Permitted pumpage (gal)	unknown	1,136,373,000	1,144,558,250	1,207,693,250	1,306,926,250	1,350,697,650	1,417,672,177	1,583,257,177	1,700,218,177
Exempt pumpage* (gal)	100,778,997	95,420,435	104,947,170	125,583,032	132,470,911	122,750,783	140,619,920	129,478,321	163,801,098
Total pumpage (gal)	unknown	1,231,793,435	1,249,505,420	1,333,276,282	1,439,397,161	1,473,448,433	1,558,292,097	1,712,735,498	1,864,019,275
Total pumpage (acre-ft)	unknown	3,780	3,834	4,091	4,417	4,521	4,782	5,255	5,720
Total pumpage (cfs)	unknown	5.2	5.3	5.7	6.1	6.2	6.6	7.3	7.9
Actual (metered) permitted pumpage	916,172,700	867,458,500	954,065,186	1,141,663,931	1,204,281,007	1,115,916,211	1,278,362,913	1,177,075,648	1,489,100,893
Exempt pumpage*	100,778,997	95,420,435	104,947,170	125,583,032	132,470,911	122,750,783	140,619,920	129,478,321	163,801,098
Total actual pumpage (gal)	1,016,951,697	962,878,935	1,059,012,356	1,267,246,963	1,336,751,918	1,238,666,994	1,418,982,833	1,306,553,969	1,652,901,991
Total pumpage (acre-ft)	3,120	2,955	3,250	3,888	4,102	3,801	4,354	4,009	5,072
Total pumpage (cfs)	4.3	4.1	4.5	5.4	5.7	5.2	6.0	5.5	7.0
Actual as a % of permitted	--	78%	85%	95%	93%	84%	91%	76%	89%

	1999	2000	2001	2002	2003	2004	2005	2006
No. Permittees	91	87	89	90	90	94	94	94
Permitted pumpage (gal)	1,754,340,569	1,777,105,569	1,936,326,800	2,154,432,800	2,182,251,250	2,383,566,187	2,464,569,937	2,469,917,445
Exempt pumpage* (gal)	150,669,960	190,030,736	197,885,377	195,092,059	194,854,638	180,449,871	208,923,973	228,441,657
Total pumpage (gal)	1,905,010,529	1,967,136,305	2,134,212,177	2,349,524,859	2,377,105,888	2,564,016,058	2,673,493,910	2,698,359,102
Total pumpage (acre-ft)	5,845	6,036	6,549	7,209	7,294	7,867	8,203	8,280
Total pumpage (cfs)	8.1	8.3	9.0	10.0	10.1	10.9	11.3	11.4
Actual (metered) permitted pumpage	1,369,726,909	1,727,552,146	1,798,957,971	1,773,564,173	1,771,405,803	1,640,453,371	1,899,308,849	2,076,742,335
Exempt pumpage*	150,669,960	190,030,736	197,885,377	195,092,059	194,854,638	180,449,871	208,923,973	228,441,657
Total actual pumpage (gal)	1,520,396,869	1,917,582,882	1,996,843,348	1,968,656,232	1,966,260,441	1,820,903,242	2,108,232,822	2,305,183,992
Total pumpage (acre-ft)	4,665	5,884	6,127	6,041	6,033	5,587	6,469	7,073
Total pumpage (cfs)	6.4	8.1	8.5	8.3	8.3	7.7	8.9	9.8
Actual as a % of permitted	80%	97%	94%	84%	83%	71%	79%	85%

* Exempt pumpage is estimated to be 11% of actual permitted pumpage.

Table 12. Water distribution material codes for the City of Austin (2016).

Pipe Materials and Symbols for the City of Austin Water Distribution System Updated: 5/24/2016	
Identification Code	**Material**
ABS	ABS truss
AC	Asbestos cement
BB	Blue brute (plastic)
C	Concrete
CI	Cast iron
CONC	Concrete
COP	Copper
CSC	Concrete steel cylinder
DI	Ductile iron
FG	Fiberglass

FRPM	Fiberglass reinforced plastic mortar
GALV	Galvanized
HDPE	High density polyethylene
PB	Polybutylene (blue plastic)
PCCP	Prestressed concrete cylinder
PE	Polyethylene
PVC	Polyvinyl chloride pipe
RC	Reinforced concrete
RCP	Reinforced concrete
STL	Steel
VC	Vitrified clay
UNK	Unknown pipe material

Appendix B

Table 13. Well withdrawal percentages by row and column for MODFLOW-GWM scenarios.

Row	Column	Percentage of Total Annual Withdrawals
10	97	0.05
9	97	0.12
8	97	0.05
99	45	1.00
101	43	2.94
4	78	0.08
91	45	2.94
58	58	0.01
76	61	5.71
75	61	0.46
92	37	0.04
81	61	5.71
92	26	0.02
72	64	0.55
99	30	0.20
61	64	0.30
68	64	0.06
62	70	0.53
61	70	0.11
11	105	0.58
48	88	0.30
104	23	10.55
43	52	0.73
85	47	0.03
86	47	0.03
22	105	0.01
23	107	1.21
61	54	0.11
75	47	1.37
69	43	0.02
68	47	0.57
91	38	0.04
84	60	1.42
71	58	0.07
48	59	3.17

65	40	0.38
62	43	0.81
7	79	0.08
78	58	1.26
65	47	0.57
30	88	0.91
66	43	0.00
65	45	0.57
61	68	0.01
81	38	0.03
78	38	0.01
57	56	0.21
60	56	0.01
69	66	1.11
61	56	0.02
65	25	0.42
44	49	0.09
101	46	0.09
109	32	8.98
99	46	6.54
52	41	0.98
51	41	0.98
101	34	1.90
88	36	0.73
91	36	6.54
92	44	2.94
97	36	0.02
65	60	0.06
63	60	0.05
64	60	0.01
93	25	0.01
67	62	0.03
107	34	6.54
64	63	0.03
83	62	0.26
58	55	0.96
56	55	0.21
51	80	0.07
45	46	0.09
60	46	0.02

102	41	0.11
61	59	0.01
60	55	0.01
68	46	0.57
60	27	0.42
82	59	0.36
71	67	4.85
71	46	1.39
64	67	0.31
77	59	1.26
56	48	0.26
58	48	0.26
66	39	0.31
66	48	3.81
62	57	0.47